
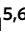








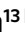





# AgRP neurons control feeding behaviour at cortical synapses via peripherally derived lysophospholipids

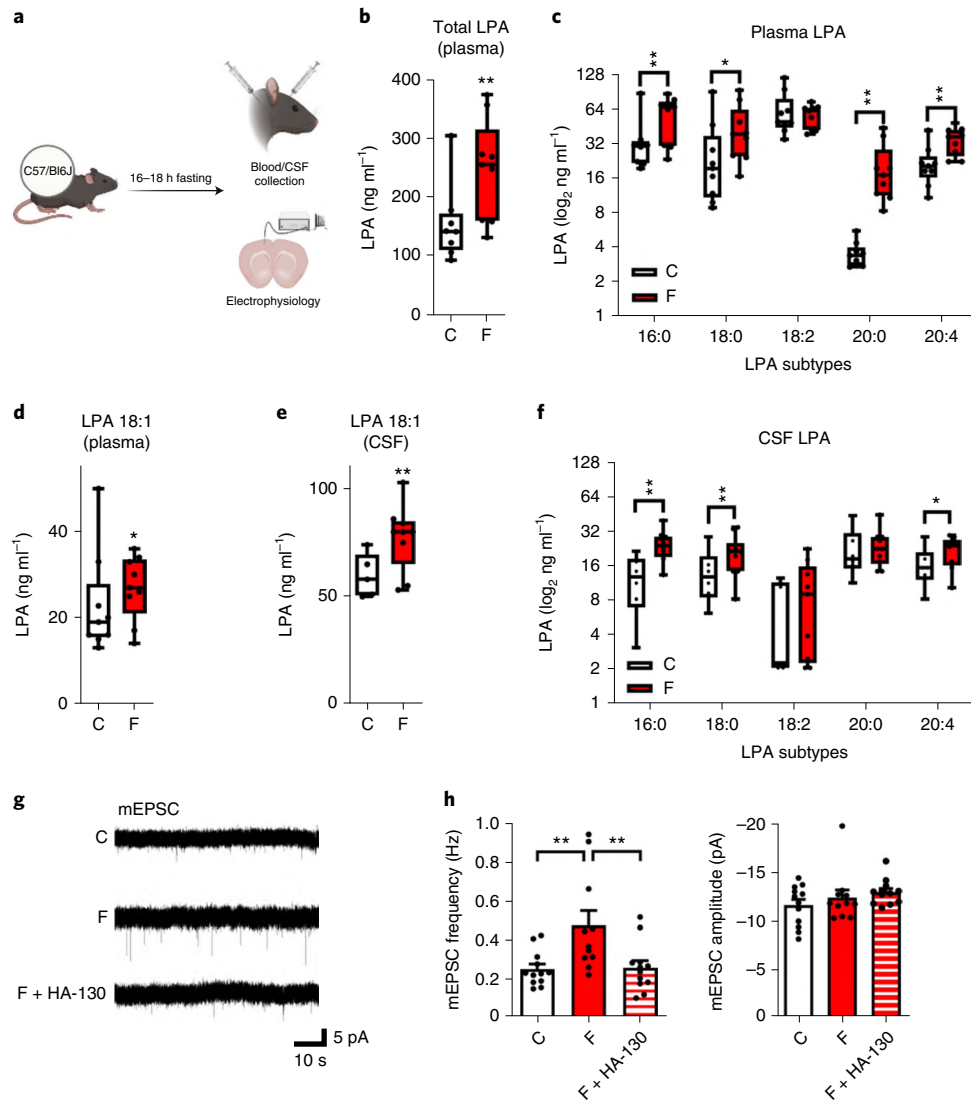
Heiko Endle <sup>1,2,3,4,15</sup>, Guilherme Horta <sup>5,6,14,15</sup>, Bernardo Stutz <sup>3,15</sup>, Muthuraman Muthuraman <sup>4</sup>, Irmgard Tegeder <sup>7</sup>, Yannick Schreiber<sup>8</sup>, Isabel Faria Snodgrass<sup>8</sup>, Robert Gurke<sup>8</sup>, Zhong-Wu Liu<sup>3</sup>, Matija Sestan-Pesa <sup>3</sup>, Konstantin Radyushkin<sup>5,6</sup>, Nora Streu<sup>5</sup>, Wei Fan <sup>5</sup>, Jan Baumgart<sup>6</sup>, Yan Li<sup>9</sup>, Florian Kloss<sup>9</sup>, Sergiu Groppa<sup>4</sup>, Nils Opel<sup>10</sup>, Udo Dannlowski<sup>10</sup>, Hans J. Grabe<sup>11</sup>, Frauke Zipp<sup>4</sup>, Bence Rácz <sup>12</sup>, Tamas L. Horvath <sup>2,3,12</sup> , Robert Nitsch <sup>13</sup>  and Johannes Vogt <sup>1,2,4</sup> 

**Phospholipid levels are influenced by peripheral metabolism. Within the central nervous system, synaptic phospholipids regulate glutamatergic transmission and cortical excitability. Whether changes in peripheral metabolism affect brain lipid levels and cortical excitability remains unknown. Here, we show that levels of lysophosphatidic acid (LPA) species in the blood and cerebrospinal fluid are elevated after overnight fasting and lead to higher cortical excitability. LPA-related cortical excitability increases fasting-induced hyperphagia, and is decreased following inhibition of LPA synthesis. Mice expressing a human mutation (*Prg-1<sup>R346T</sup>*) leading to higher synaptic lipid-mediated cortical excitability display increased fasting-induced hyperphagia. Accordingly, human subjects with this mutation have higher body mass index and prevalence of type 2 diabetes. We further show that the effects of LPA following fasting are under the control of hypothalamic agouti-related peptide (AgRP) neurons. Depletion of AgRP-expressing cells in adult mice decreases fasting-induced elevation of circulating LPAs, as well as cortical excitability, while blunting hyperphagia. These findings reveal a direct influence of circulating LPAs under the control of hypothalamic AgRP neurons on cortical excitability, unmasking an alternative non-neuronal route by which the hypothalamus can exert a robust impact on the cortex and thereby affect food intake.**

Recent research has shown that bioactive phospholipids such as lysophosphatidic acids play an important regulatory role in synaptic neurotransmission and plasticity<sup>1–4</sup>. LPA is a short-lived, but potent, signalling molecule<sup>5</sup> that acts via specific G-protein-coupled receptors, LPA-R<sub>1–6</sub> (refs. <sup>6,7</sup>). LPA levels are tightly regulated by specific phosphatases (LPP<sub>1–3</sub> (ref. <sup>8</sup>)), suggesting that LPA synthesis and action are locally restricted. We have previously shown that LPA is locally synthesized at the synaptic cleft of glutamatergic synapses by autotaxin (*ATX/Enpp2* (refs. <sup>9–11</sup>)), which is expressed by astrocytic processes covering cortical glutamatergic synapses<sup>4</sup>. Here, LPA is a powerful modulator of presynaptic glutamate release by activation of presynaptic LPA<sub>2</sub> receptors, which regulate glutamate release probabilities and thereby neuronal excitability<sup>1</sup>. In cortical networks, LPA regulates the cortical excitation/inhibition (E/I) balance and controls cortical sensory information processing in mice and humans<sup>3</sup>.

LPA synthesis in the brain depends on the presence of its precursor lysophosphatidyl choline (LPC), which is secreted by the liver and reflects changes in peripheral energy metabolism<sup>12,13</sup> and is actively transported via the blood–brain barrier<sup>14</sup>. However, in contrast to blood plasma, LPC is present at only very low concentrations in cerebral spinal fluid (CSF)<sup>6,15,16</sup>, indicating that LPC levels may be a limiting factor for LPA synthesis in the central nervous system. Taken together, these findings suggest that changes in peripheral energy metabolism may affect brain lipid levels and thereby cortical excitability. Because food restriction rapidly depletes glycogen stores and induces lipolysis, thereby altering body lipid levels<sup>17</sup>, and AgRP neurons have been shown to control peripheral lipid metabolism<sup>18,19</sup> and complex behaviours beyond feeding<sup>19–21</sup>, we interrogated the effect of fasting and AgRP circuit integrity on brain phospholipid levels, as well as its impact on both cortical excitability and food intake control.

<sup>1</sup>Department of Molecular and Translational Neuroscience of Anatomy II, University of Cologne, Cologne, Germany. <sup>2</sup>Cluster of Excellence-Cellular Stress Response in Aging-Associated Diseases, Center of Molecular Medicine Cologne, University of Cologne, Cologne, Germany. <sup>3</sup>Department of Comparative Medicine, Yale School of Medicine, New Haven, CT, USA. <sup>4</sup>Department of Neurology, Focus Program Translational Neuroscience (FTN) and Immunotherapy (FZI), Rhine Main Neuroscience Network (rmn2), University Medical Center of the Johannes Gutenberg-University, Mainz, Germany. <sup>5</sup>Focus Program Translational Neuroscience, Johannes Gutenberg-University, Mainz, Germany. <sup>6</sup>Translational Animal Research Center, University Medical Center of the Johannes Gutenberg-University, Mainz, Germany. <sup>7</sup>Institute of Clinical Pharmacology, Goethe-University, Frankfurt am Main, Germany. <sup>8</sup>Fraunhofer Institute for Translational Medicine and Pharmacology and Fraunhofer Cluster of Excellence for Immune Mediated Diseases, Frankfurt am Main, Germany. <sup>9</sup>Transfer Group Antiinfectives, Leibniz Institute for Natural Product Research and Infection Biology, Hans Knöll Institute, Jena, Germany. <sup>10</sup>Institute of Translational Psychiatry, Westfälische Wilhelms University, Münster, Germany. <sup>11</sup>Department of Psychiatry and Psychotherapy, University Medicine Greifswald, Greifswald, Germany. <sup>12</sup>Department of Anatomy and Histology, University of Veterinary Medicine, Budapest, Hungary. <sup>13</sup>Institute for Translational Neuroscience, Westfälische Wilhelms University, Münster, Germany. <sup>14</sup>Present address: Institute for Microscopic Anatomy and Neurobiology, Johannes Gutenberg-University, Mainz, Germany. <sup>15</sup>These authors contributed equally: Heiko Endle, Guilherme Horta, Bernardo Stutz. ✉e-mail: [tamas.horvath@yale.edu](mailto:tamas.horvath@yale.edu); [nitschr@uni-muenster.de](mailto:nitschr@uni-muenster.de); [johannes.vogt@uk-koeln.de](mailto:johannes.vogt@uk-koeln.de)



**Fig. 1 | Fasting increases synaptic active LPA subtypes in the brain and enhances glutamatergic transmission.** **a**, Experimental design for blood plasma and CSF collection. **b**, Total LPA blood plasma levels were increased in WT animals after fasting ( $n=8$  control (C) animals and  $n=9$  fasted (F) animals; group differences, 97.8% by Bayesian analysis). **c**, LPA subtype analysis revealed increased blood plasma levels in fasted WT ( $n=9$  controls for LPA 18:0, 18:2, 20:0, 20:4,  $n=8$  for LPA 16:0 and  $n=9$  fasted animals; group differences for LPA 16:0, 18:0, 18:2, 20:0 and 20:4 were 97.1, 89.9, 60.9, 99.7 and 99.1%, respectively, by Bayesian analysis). **d**, Blood plasma levels of LPA 18:1 were increased in fasted WT animals ( $n=9$  control animals and  $n=9$  fasted animals; group differences 83.8% by Bayesian analysis). **e**, Fasting resulted in increased CSF LPA 18:1 levels ( $n=5$  control animals and  $n=9$  fasted animals; group differences 96.4% by Bayesian analysis). **f**, In CSF, fasting increased specific LPA levels ( $n=6$  controls for LPA 16:0, 18:0, 20:0, 20:4 and  $n=5$  for 18:2;  $n=10$  fasted animals for LPA 16:0, 18:0, 20:0, 20:4 and  $n=9$  for LPA 18:2; group differences for LPA 16:0, 18:0, 18:2, 20:0 and 20:4 were 98.7, 90.3, 76.9, 60.0 and 89.2%, respectively, by Bayesian analysis). **g**, Original mEPSC traces illustrating presynaptic release probabilities under control conditions, after fasting (F) and after application of the ATX inhibitor HA-130 after fasting (F + HA-130). **h**, mEPSC frequencies were significantly increased after fasting (F,  $P=0.0058$ ) and were reduced to control values (C) when ATX was inhibited by HA-130 (F + HA-130,  $P=0.0077$ ) ( $n=12$  for C,  $n=11$  for F,  $n=12$  for F + HA-130; one-way analysis of variance (ANOVA) with Bonferroni correction (frequencies, left) or Kruskal-Wallis test (amplitudes, right)). Bars represent mean + s.e.m. Box plots and whiskers show data from minimum to maximum, line shows median; points represent individual values. \*\* $P < 0.01$  for group differences of  $>80\%$  (\*) or  $>90\%$  (\*\*) for Bayesian analysis. Credit: illustration in **a** was created with BioRender.com.

## Results

**Fasting increases cortical excitability via synaptic lipid signaling.** Overnight fasting of mice is sufficient to deplete liver glycogen content, significantly reducing blood glucose levels and inducing liver lipolysis and lipid secretion into the blood<sup>17</sup>. One lipid secreted by the liver is LPC, which is rapidly converted to LPA by ATX, an enzyme that is abundantly present in blood<sup>11</sup>. We analysed fasting-induced LPA levels (experimental scheme in Fig. 1a) and found that overnight fasting resulted in increased blood plasma

levels, as well as an increase in LPA subtypes (Fig. 1b,c). Moreover we found higher levels of LPA 18:1, which is described as having a high affinity to the presynaptic LPA<sub>2</sub> receptor<sup>22</sup> and as being a potent mediator in the periphery<sup>23</sup> (Fig. 1d). Further CSF analysis revealed substantially increased LPA levels, including LPA 18:1, after overnight fasting (Fig. 1e,f).

Because increases in synaptic LPA have been associated with higher miniature excitatory postsynaptic current (mEPSC) frequencies, which reflect glutamatergic release probabilities<sup>1,2</sup>, we assessed

mEPSCs in hippocampal neurons, which are located in regions with high expression of both the LPA-synthesizing molecule ATX and the LPA-interacting molecule PRG-1 (for expression of *Atx* and *Prg-1* see Extended Data Fig. 1a–j). First we measured mEPSCs in fasted animals, finding significantly increased mEPSC frequencies after overnight fasting (Fig. 1g,h). To interrogate that the above described changes in cortical excitability were the result of increased LPA, we inhibited LPA synthesis at the synaptic cleft by application of HA-130, blocking the LPA-synthesizing enzyme ATX, which is released from perisynaptic astrocyte processes<sup>4</sup>. In fact, we have previously shown that HA-130 decreased mEPSC frequencies to control values under conditions of hyperexcitability while not affecting mEPSCs under control conditions<sup>4</sup>. HA-130 application after fasting resulted in mEPSC frequencies at control levels (Fig. 1g,h). Because unsaturated LPA subtypes such as LPA 18:1 have a preference for LPA<sub>2</sub> receptors<sup>22</sup>, and this LPA subtype was increased after fasting, we tested the action of LPA 18:1 on presynaptic glutamatergic release probabilities. LPA 18:1 significantly enhanced mEPSC frequencies (Extended Data Fig. 2a–c) while saturated LPA 18:0 resulted in no significant changes (Extended Data Fig. 2d–f). This is consistent with previous *in vitro* reports using LPA receptor expression in heterologous systems<sup>22</sup>. These data show, therefore, that during fasting, synaptically active LPA subtype levels such as LPA 18:1 (acting via presynaptic LPA<sub>2</sub>-R as described<sup>1,22</sup>) were enhanced in the brain, leading to increased cortical excitability.

#### **Fasting-related cortical excitability affects exploratory behaviour.**

According to the high expression of LPA-modulating molecules ATX and PRG-1 in the upper cortical layers (shown also in Extended Data Fig. 1), we assessed the effect of fasting on increased cortical excitability in a cortex-related behaviour. Here, we tested the exploratory behaviour of mice exposed to a novel, non-food-related object<sup>24</sup>, finding a significantly longer interaction time for fasted animals exposed to the novel object (Extended Data Fig. 3b). However, inhibition of the LPA synthesis molecule ATX by PF8380, which significantly reduced synaptic active LPA 18:1 levels in CSF (Extended Data Fig. 4b), completely blunted the fasting-induced exploratory drive (Extended Data Fig. 3b) while it did not affect basic motor function (Extended Data Fig. 4c). To confirm the involvement of fasting-related LPA changes in the cortex, we disrupted cortical LPA signalling (*Atx<sup>Δcortex</sup>* using a cortex-specific *Emx1-Cre* mouse line). Cortical ATX disruption resulted in decreased exploratory behaviour after fasting, while no differences were observed under control conditions (Extended Data Fig. 3c). Interestingly, following cortical ATX disruption, exploratory drive was not significantly different between non-fasted and fasted mice (Extended Data Fig. 3d) and was no longer affected by ATX inhibition (Extended Data Fig. 3e). To summarize, these data suggest that fasting-induced exploratory behaviour is modulated by cortical ATX. To further confirm the impact of synaptic LPA signalling on exploratory behaviour, we assessed the role of the downstream presynaptic LPA<sub>2</sub> receptor, which has been shown to mediate LPA-related cortical excitability<sup>1</sup>. Here, exploratory behaviour of fasted LPA<sub>2</sub> receptor knockout mice (*Lpa2<sup>-/-</sup>*) was significantly lower than in their wild-type (WT) litters, while no difference was observed either under non-fasted conditions or after ATX inhibition (Extended Data Fig. 3f,g).

Finally, we tested whether a pre-existing, synaptic LPA-related increase in cortical excitability would be able to potentiate fasting-induced, cortex-related behaviour. To do this we assessed the exploratory behaviour of fasted *Prg-1<sup>R346T/+</sup>* mice, which express a monoallelic single-nucleotide polymorphism (SNP) in the plasticity-related gene (*Prg-1/Lppr4*), as described in humans<sup>3</sup>. This SNP (with a population frequency of around 0.6% in humans) leads to a single amino acid change (PRG-1<sup>R346T</sup>), resulting in loss of the ability of PRG-1 to take up LPA and clear it from the synaptic cleft, which would thus lead to increased synaptic LPA signalling and

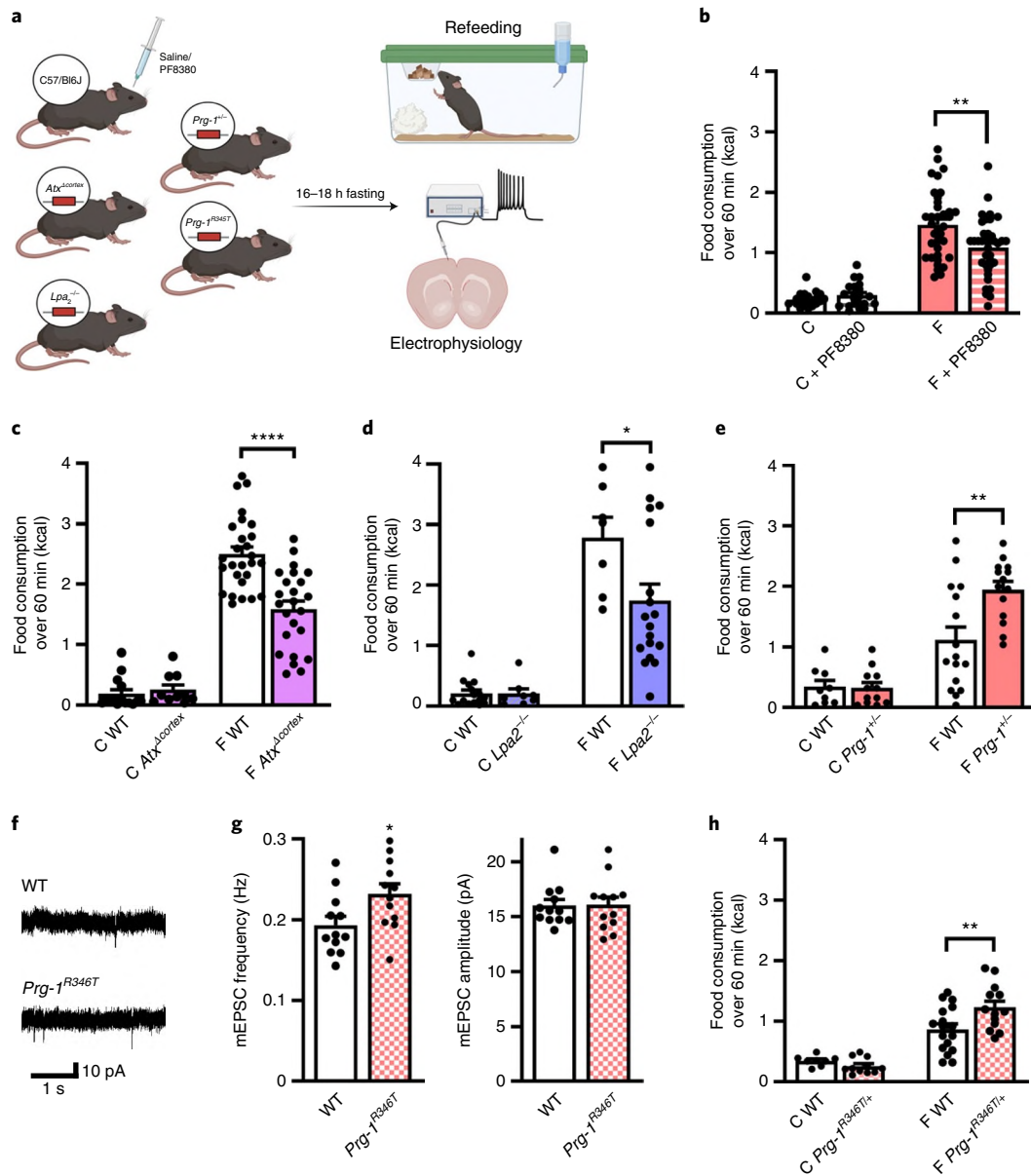
altered glutamatergic transmission<sup>3,4</sup>. Overnight fasted *Prg-1<sup>R346T/+</sup>* mice showed a significant increase in exploration time compared with their fasted WT litters (Extended Data Fig. 3h). In line with the predominant cortical PRG-1 expression on glutamatergic neurons, and due to the fact that the human PRG-1<sup>R345T</sup> variant is a loss-of-function mutation selectively affecting the ability to remove LPA from the synaptic cleft<sup>3</sup>, these data suggest that, following fasting, increased synaptic LPA signalling in the cortex leads to a higher exploratory drive which, in the normal habitat of an animal, is part of food-searching activity.

#### **LPA-modulated cortical excitability influences fasting-induced hyperphagia.**

Fasting-induced hyperphagia is a well-described phenomenon leading to rapid reversal of fasting-induced changes in peripheral energy metabolism<sup>17</sup>. While part of the effect of fasting-induced hyperphagia is associated with ghrelin signalling<sup>25</sup> or specific potassium currents in hypothalamic neurons<sup>26</sup>, the role of higher-order cortical regulation—as well as that of the underlying metabolic signalling pathway—remain unclear. Because we found synaptic lipid signalling to be modulated by changes in peripheral energy metabolism, we assessed the effect of ATX inhibition by PF8380 on fasting-induced hyperphagia (schematic experimental overview shown in Fig. 2a). ATX inhibition by PF8380 significantly decreased fasting-induced hyperphagia when compared with non-treated fasted mice, while ATX inhibition had no effect on food intake under non-fasted conditions (Fig. 2b). This cortex-dominated action was corroborated by cortical deletion of the LPA-synthesizing molecule ATX (*Atx<sup>Δcortex</sup>* mice), as well as by deletion of the LPA<sub>2</sub> receptor (*Lpa2<sup>-/-</sup>* mice), both of which have previously been reported to reduce LPA-related cortical excitability to WT levels<sup>1,4</sup>. Here we observed a significant reduction in fasting-induced hyperphagia after disruption of the ATX–LPA–LPA<sub>2</sub> signalling axis when compared with WT litters, while food intake in these transgenic mouse lines was no different to that in their WT litters under non-fasting conditions (Fig. 2c,d), suggesting that the ATX–LPA–LPA<sub>2</sub> signalling axis is activated under altered metabolic conditions.

Next, we tested whether a pre-existing, synaptic LPA-related increase in cortical excitability could potentiate fasting-induced hyperphagia. To accomplish this, we assessed *Prg-1<sup>+/-</sup>* animals, which have previously been shown to display a gene-dosage effect leading to 50% reduction in PRG-1 protein levels, resulting in cortical hyperexcitability midway between that of WT and *Prg-1<sup>-/-</sup>* animals<sup>4</sup>. Here, *Prg-1<sup>+/-</sup>* animals showed a significant increase in fasting-induced hyperphagia when compared with their WT litters, while food intake was not altered under non-fasting conditions (Fig. 2e). To assess the translational potential of our findings, we next assessed fasting-induced hyperphagia in *Prg-1<sup>R346T/+</sup>* mice. Loss of PRG-1 synaptic function, as induced by the *Prg-1<sup>R346T</sup>* SNP, would thus lead to increased synaptic LPA signalling and augmented glutamatergic transmission<sup>3,4</sup>. To test for this, we first assessed mEPSCs in PRG-1<sup>R346T</sup> animals. We detected increased glutamatergic release probability, pointing to a constitutively higher cortical network excitability under baseline conditions (Fig. 2f,g). *Prg-1<sup>R346T/+</sup>* mice displayed a significant increase in fasting-induced hyperphagia comparable to that in *Prg-1<sup>R346T/+</sup>* animals, indicating a critical role of LPA-mediated cortical excitability in food intake control (Fig. 2h and Extended Data Fig. 5a). To exclude the possibility that our observations might have been influenced by secondary effects such as altered locomotion, we assessed spontaneous locomotion of non-fasted and fasted animals in an open-field setting. Here, we observed no significant changes in locomotion after 18 h of fasting (Extended Data Fig. 4c–f), which is in line with data from other groups for a similar fasting period<sup>27</sup>.

To summarize, our observations may thus point to a causal relationship between cortical hyperexcitability in human subjects with



**Fig. 2 | Fasting-induced hyperphagia is regulated by cortical synaptic lipid signalling.** **a**, Experimental design. **b**, Disruption of LPA signalling via systemic ATX inhibition (by PF8380) did not alter food intake under non-fasting conditions ( $n=20$  C,  $n=21$  C + PF8380, Mann-Whitney test), while ATX inhibition significantly reduced fasting-induced hyperphagia ( $n=36$  F,  $n=37$  F + PF8380,  $P=0.0028$ , two-tailed  $t$ -test), while fasting-induced hyperphagia was significantly reduced in  $Atx^{\Delta cortex}$  mice when compared with their WT litters ( $n=27$  F WT,  $n=24$  F  $Atx^{\Delta cortex}$  mice,  $P<0.0001$ , two-tailed  $t$ -test). **c**, Food intake under control conditions was comparable in non-fasted WT and  $Atx^{\Delta cortex}$  mice ( $n=15$  C WT,  $n=10$  C  $Atx^{\Delta cortex}$ , two-tailed  $t$ -test), while fasting-induced hyperphagia was significantly reduced in  $Atx^{\Delta cortex}$  mice when compared with their WT litters ( $n=7$  F WT,  $n=18$  F  $Atx^{\Delta cortex}$  mice,  $P=0.031$ , two-tailed  $t$ -test). **d**, Food intake under control conditions was not different in  $Lpa2^{-/-}$  mice compared with that in their WT litters ( $n=16$  C WT,  $n=8$  C  $Lpa2^{-/-}$ ), although fasting-induced hyperphagia was significantly reduced in  $Lpa2^{-/-}$  mice compared with that in their WT litters ( $n=7$  F WT,  $n=18$  F  $Lpa2^{-/-}$  mice,  $P=0.031$ , two-tailed  $t$ -test). **e**, Food consumption under non-fasted, control conditions was similar in PRG-1 $^{+/-}$  ( $n=12$ ) and their WT litters ( $n=9$ , two-tailed  $t$ -test); however, after overnight fasting, fasting-induced hyperphagia was significantly increased in PRG-1 $^{+/-}$  mice compared with that in their WT litters ( $n=16$  fasted WT,  $n=14$  fasted PRG-1 $^{+/-}$  mice,  $P=0.003$ , two-tailed  $t$ -test). **f**, Original traces of mEPSCs from PRG-1 $^{R346T}$  mice and WT litters. **g**, mEPSC showed significantly increased mEPSC frequencies with unaltered amplitudes in PRG-1 $^{R346T}$  mice ( $n=12$  WT,  $n=12$  PRG-1 $^{R346T}$  mice,  $P=0.028$ , two-tailed  $t$ -test). **h**, Under non-fasting, control conditions food intake was not different between mice expressing human PRG-1 $^{R346T}$  SNP (PRG-1 $^{R346T/+}$  mice) and their WT litters ( $n=8$  C WT,  $n=11$  C PRG-1 $^{R346T/+}$ ). After fasting, however, PRG-1 $^{R346T/+}$  mice displayed significantly increased fasting-induced hyperphagia when compared with their WT litters ( $n=17$  F WT,  $n=13$  F PRG-1 $^{R346T/+}$  mice,  $P=0.007$ , one-tailed  $t$ -test). Bars represent mean + s.e.m., points represent individual values. \* $P<0.05$ , \*\* $P<0.01$ , \*\*\*\* $P<0.0001$ . Credit: illustration in **a** was created with [BioRender.com](https://www.biorender.com).

eating disorders, because successful therapeutic intervention modulating cortical excitability was shown in these subjects by repeated transcranial magnetic stimulation and transcranial direct current stimulation<sup>28</sup>.

**Synaptic lipid signalling modulates food intake and body weight.** Because LPA-related cortical excitability modulates fasting-induced hyperphagia, we assessed the role of cortical excitability in long-term body weight changes (experimental setting shown in

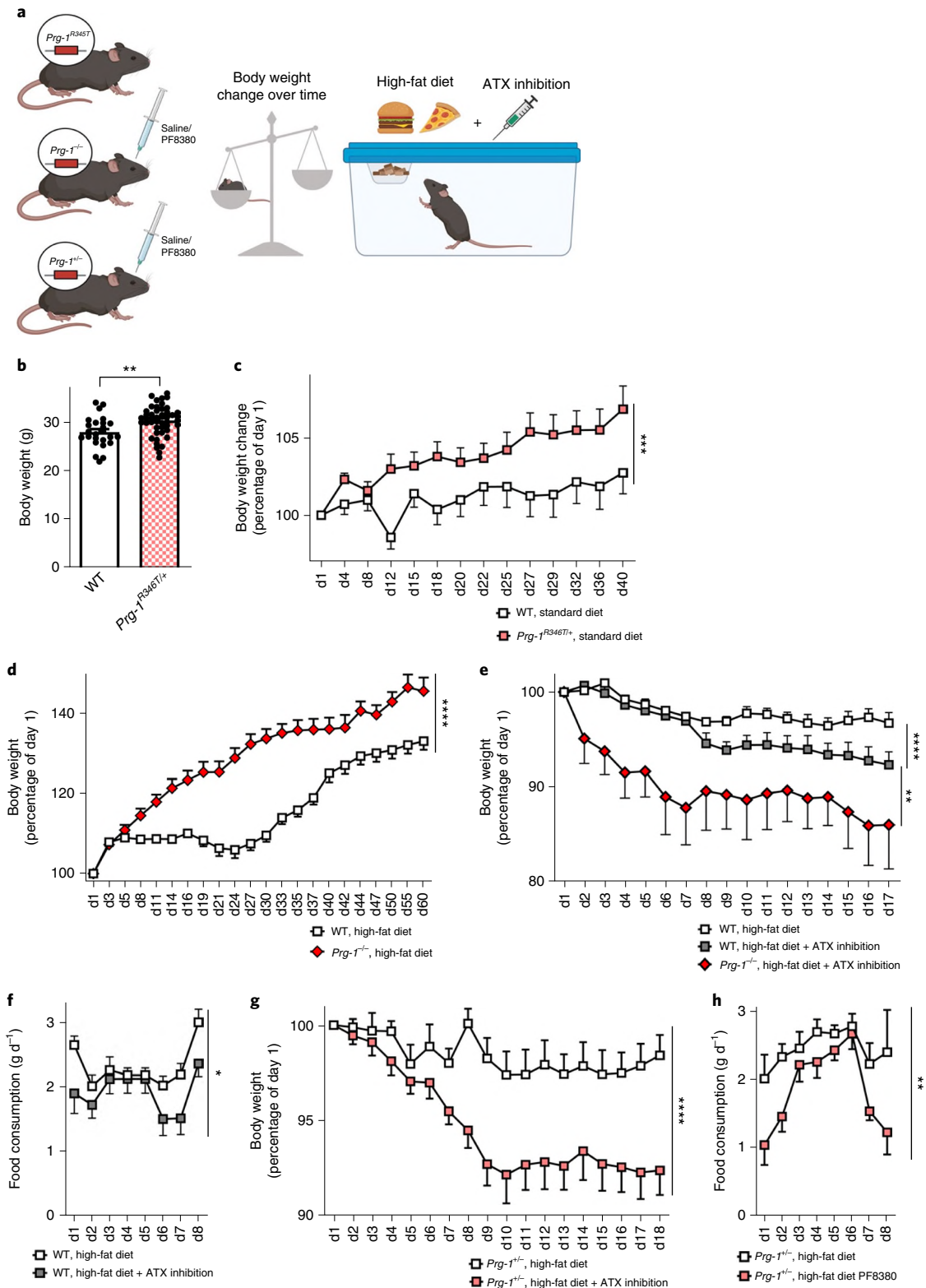


Fig. 3a). Already under standard diet conditions, *Prg-1<sup>R346T/+</sup>* mice displayed significantly higher body weight (Fig. 3b). Regular body weight assessed over 6 weeks confirmed significant higher body weight increase in *Prg-1<sup>R346T/+</sup>* mice when compared with WT animals (Fig. 3c). Food intake assessment under control conditions over a full 24h period revealed higher food intake in *Prg-1<sup>R346T/+</sup>* mice when compared with WT littermates (Extended data Fig. 5b). To assess the translational potential of this finding we assessed

human *PRG-1<sup>R345T/+</sup>* mutation carriers, finding a higher body mass index (BMI) and higher prevalence for diabetes mellitus type II (Extended Data Fig. 5c,d). These data suggest that higher synaptic lipid-induced cortical excitability in *PRG-1<sup>R345T/+</sup>* mutation carriers leading to putative higher food intake has long-term effects in humans, resulting in higher BMI associated with metabolic disorders such as diabetes mellitus type II. To clarify the role of higher cortical excitability in more detail, we assessed body weight changes

**Fig. 3 | Synaptic lipid signalling modulates body weight under both control and high-fat diets.** **a**, Experimental design. **b**, *Prg-1<sup>TR346T/+</sup>* (17.1 ± 3 weeks) mice displayed significantly higher body weight than WT of a similar age (WT, 16.9 ± 3 weeks) ( $n = 25$  WT mice,  $n = 46$  *Prg-1<sup>TR346T/+</sup>* mice,  $P = 0.0032$ , two-sided *t*-test). **c**, Body weight changes over 6 weeks (±1 day starting around 17 weeks; d1, day 1) on standard diet revealed a higher increase in *Prg-1<sup>TR346T/+</sup>* animals ( $n = 25$  WT,  $n = 31$  *Prg-1<sup>TR346T/+</sup>* mice, two-way ANOVA,  $P = 0.0008$  for days on standard food × genotype). **d**, *Prg-1<sup>-/-</sup>* animals showed greater increase in body weight when administered a high-fat diet compared with WT mice ( $n = 27$  WT mice,  $n = 12$  *Prg-1<sup>-/-</sup>* mice, two-way repeated measures (RM) ANOVA,  $P < 0.0001$ , days on high-fat diet × genotype). **e**, ATX inhibition by PF8380 under continuation of high-fat diet resulted in significant weight loss in WT animals compared with non-treated WT animals. However, *Prg-1<sup>-/-</sup>* animals under ATX inhibition by PF8380 displayed significantly higher weight loss than WT mice ( $n = 13$  WT,  $n = 14$  WT + PF8380 animals,  $n = 5$  *Prg-1<sup>-/-</sup>* + PF8380 animals,  $P < 0.0001$ , two-way RM ANOVA, time × PF8380 treatment for WT versus WT + PF8380; PF-8389 treatment × genotype for WT + PF8380 and *Prg-1<sup>-/-</sup>* + PF8380,  $P = 0.008$ , two-way RM ANOVA). **f**, Food intake under ATX inhibition by PF8380 was significantly reduced in WT mice ( $n = 13$  controls,  $n = 14$  PF8380-treated WT animals, two-way RM ANOVA,  $P = 0.044$ , PF8380 treatment). **g**, Following administration of a high-fat diet, ATX inhibition by PF8380 under continuation of high-fat diet resulted in significant body weight reduction in treated *Prg-1<sup>-/-</sup>* mice compared with non-treated *Prg-1<sup>-/-</sup>* mice ( $n = 16$  *Prg-1<sup>-/-</sup>* mice,  $n = 18$  *Prg-1<sup>-/-</sup>* PF8380-treated mice, two-way RM ANOVA,  $P < 0.0001$ , time × PF8380 treatment). **h**, Food intake in *Prg-1<sup>-/-</sup>* animals was significantly reduced following ATX inhibition by PF8380 ( $n = 9$  *Prg-1<sup>-/-</sup>* mice,  $n = 9$  *Prg-1<sup>-/-</sup>* PF8380-treated mice, two-way RM ANOVA,  $P = 0.0076$ , PF8380 treatment). Dots indicate single values, bars represent mean and error bars represent s.e.m., which are shown for better visibility in **c-h** in one direction only. \* $P < 0.05$ , \*\* $P < 0.01$ , \*\*\* $P < 0.001$ , \*\*\*\* $P < 0.0001$ . Credit: illustration in **a** was created with [BioRender.com](https://www.biorender.com).

in WT and *Prg-1<sup>-/-</sup>* animals under a high-fat diet, finding significant body weight increase in the latter when compared with the former (Fig. 3d). Although ATX inhibition significantly reduced body weight in WT animals under continuation of high-fat diet, it led to significantly higher body weight reduction in *Prg-1<sup>-/-</sup>* animals when compared with their WT litters (Fig. 3e). Assessment of food intake suggests that the observed weight loss could be attributed to lower food intake in PF8380-treated WT animals when compared with non-treated litters (Fig. 3f). These data were confirmed in *Prg-1<sup>+/-</sup>* animals on a high-fat diet, which displayed significant body weight reduction and lower food intake under PF8380 treatment (Fig. 3g,h). However, pharmacological assessment of PF8380 showed the rapid appearance of a metabolic product suggesting its relatively low metabolic stability (Extended Data Fig. 5e,f).

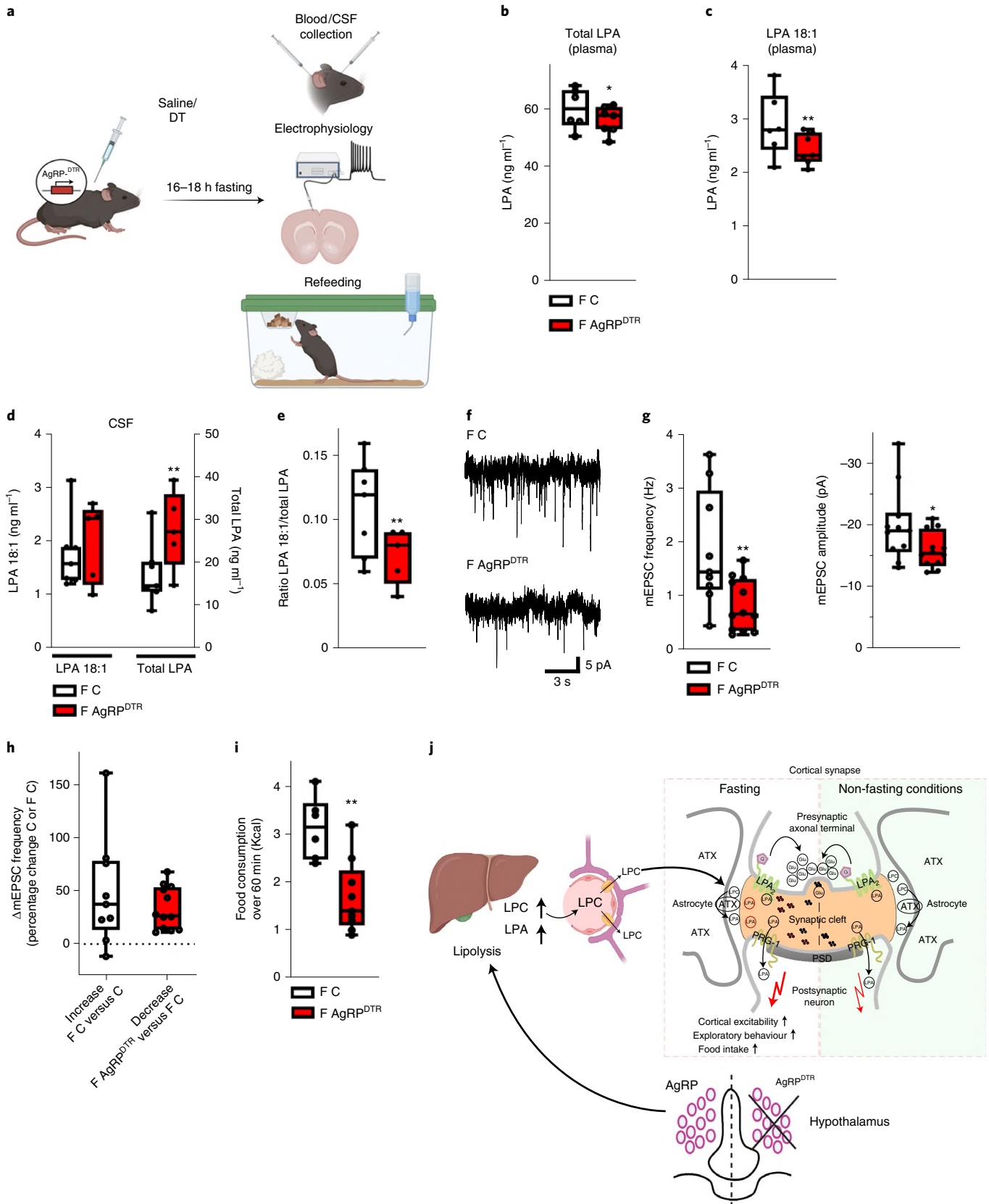
**Fasting-induced cortical excitability via synaptic lipid signalling relies on AgRP circuit integrity.** Neuropeptide Y/AgRP-expressing neurons in the hypothalamic arcuate nucleus are critical for peripheral lipid mobilization and complex behaviours during food-restricted periods<sup>19</sup>. As a result, we next tested whether hypothalamic AgRP circuit integrity is involved in fasting-associated LPA changes. We analysed LPA levels in the blood plasma of fasted controls and fasted animals following diphtheria toxin (DT) ablation of AgRP neurons expressing the DT receptor (AgRP<sup>DTTR</sup>)<sup>29</sup>. While under fed conditions, neither control nor AgRP<sup>DTTR</sup> mice

showed any differences in blood free fatty acids as shown previously in peri-adolescence<sup>19</sup>; after fasting, we found reduced total LPC and total LPA plasma levels, as well as diminished LPC 18:1 and LPA 18:1 levels in the blood plasma of fasted DT-treated AgRP<sup>DTTR</sup> animals when compared with fasted control animals (saline-treated AgRP<sup>DTTR</sup> mice; Fig. 4b,c and Extended Data Fig. 6a,b). In addition, we analysed CSF levels of both synaptically active LPA 18:1 and total LPA. Since high inter-individual variations may obscure group differences in regard to single metabolites<sup>30</sup> and, due to the high variation in total CSF LPA levels in the analysed animals (Fig. 4d and Extended Data Fig. 6c,d), LPA 18:1 levels were calculated as the ratio to total CSF LPA levels as previously described by others<sup>31,32</sup>. Here, we found a significantly reduced ratio of LPA 18:1 to total LPAs as well as a reduction in the ratio of other LPA subtypes in the CSF of AgRP<sup>DTTR</sup> mice compared with control animals (Fig. 4e and Extended Data Fig. 6e). This ratiometric data allows for a functional understanding of phospholipid effects at the synapse where high levels of other LPA subtypes may outcompete LPA 18:1. Because the LPA-modulatory molecules ATX and PRG-1 are well expressed in the upper layers of the prefrontal cortex (Extended Data Fig. 7), we assessed mEPSCs in the prefrontal cortex (layers II/III) of fasted control and fasted AgRP neuron-ablated animals (AgRP<sup>DTTR</sup>). Here, we detected significant lower frequencies and lower amplitudes of mEPSCs on cortical principal cells of fasted AgRP<sup>DTTR</sup> mice compared with controls (Fig. 4f,g), indicating reduced fasting-induced

**Fig. 4 | Fasting-induced hyperphagia depends on AgRP circuit integrity.** **a**, Experimental design. **b**, Total LPA blood plasma levels were significantly decreased in fasted AgRP<sup>DTTR</sup> (F AgRP<sup>DTTR</sup>) mice ( $n = 6$  fasted controls (FC),  $n = 7$  fasted AgRP<sup>DTTR</sup> mice, group differences 81.0%, Bayesian analysis). **c**, Analysis revealed reduced plasma LPA 18:1 levels in fasted AgRP<sup>DTTR</sup> mice ( $n = 6$  FC,  $n = 7$  F AgRP<sup>DTTR</sup> mice, group differences 90.5%, Bayesian analysis). **d**, CSF LPA 18:1 levels were comparable in fasted AgRP<sup>DTTR</sup> mice and fasted control animals (left, group differences 70.0%) while total LPA levels were significantly increased in fasted AgRP<sup>DTTR</sup> mice, displaying high variation ( $n = 7$  fasted control mice,  $n = 5$  fasted AgRP<sup>DTTR</sup> mice, group differences 92.6%, Bayesian analysis). **e**, CSF levels of synaptic active LPA 18:1, calculated as ratio to total CSF LPA levels in corresponding animals, showed significant reduction in fasted AgRP<sup>DTTR</sup> mice ( $n = 7$  fasted control mice,  $n = 5$  fasted AgRP<sup>DTTR</sup> mice, group differences 93.5%, Bayesian analysis). **f**, Original traces displaying mEPSCs from prefrontal cortical neurons from FC and fasted, DT-treated AgRP<sup>DTTR</sup> animals (F AgRP<sup>DTTR</sup>). **g**, mEPSC frequency and amplitude were reduced in neurons of fasted AgRP<sup>DTTR</sup> animals ( $n = 9$  (frequency),  $n = 11$  (amplitude) of FC,  $n = 12$  fasted AgRP<sup>DTTR</sup> mice,  $P = 0.0077$  for frequency and  $P = 0.044$  for amplitude, two-sided *t*-test). **h**, mEPSC changes in fasted controls ( $n = 9$  FC increase compared with mean of non-fasted controls shown in Fig. 1h) and fasted AgRP<sup>DTTR</sup> animals ( $n = 12$  F AgRP<sup>DTTR</sup> reduction compared with mean of FC shown in Fig. 4g, two-sided Mann-Whitney test) did not reveal significant differences. **i**, Fasting-induced hyperphagia was significantly decreased in AgRP<sup>DTTR</sup> mice ( $n = 6$  FC,  $n = 9$  F AgRP<sup>DTTR</sup>,  $P = 0.0022$ , two-tailed *t*-test). **j**, Scheme of fasting-induced increase in cortical excitability by peripherally produced LPA precursors. Following overnight fasting, glycogen stores in the liver are depleted and lipolysis is increased leading to LPC release in the blood, causing increased LPA levels after overnight fasting via ATX-dependent synthesis in the blood. Our data suggest that this first step in metabolic adaptation to fasting conditions is regulated by AgRP neurons in the hypothalamus. However, following peripheral release upon fasting, LPC is selectively transported across the blood-brain barrier and is metabolized by astrocytic ATX at glutamatergic synapses to generate local LPA, which stimulates presynaptic LPA2 receptors leading to fasting-induced increase in glutamatergic transmission and cortical network excitability. In turn, fasting-induced cortical excitability drives fasting-induced hyperphagia, as shown by the present data. Box plots and whiskers show data from minimum to maximum, line shows median, points represent individual values. \* $P < 0.05$ , \*\* $P < 0.01$  or group differences of \* $>80\%$  or \*\* $>90\%$  for Bayesian analysis. Credit: illustrations in **a,j** were created with [BioRender.com](https://www.biorender.com).

cortical excitability in  $\text{AgRP}^{\text{DTR}}$  animals. To assess the magnitude of the effect of hypothalamic  $\text{AgRP}$  depletion on fasting-induced increase in cortical excitability, we compared the reduction of mEPSCs in fasted  $\text{AgRP}^{\text{DTR}}$  mice (when compared with mEPSCs of fasted controls) to mEPSC increase in fasted control mice (when compared

with mEPSCs of non-fasted mice), finding no significant difference (Fig. 4h). These data indicate that fasting-induced increase in LPA depends on  $\text{AgRP}$  neuronal activity leading to increased probability of presynaptic glutamatergic release which, in turn, results in increased cortical network excitability. This synaptic lipid signalling



has been shown to play a role in psychiatric disorders<sup>1–4</sup>, and our data may also be relevant in regard to other altered complex behaviours, including stereotypy and anorexia nervosa symptomatology in mice with altered AgRP neuronal activity at different ages<sup>19,21</sup>.

**Fasting-induced hyperphagia is dependent on AgRP circuit integrity.** Finally, in support of the above datasets, we assessed fasting-related hyperphagia in control and AgRP<sup>DTR</sup> animals. While under control conditions (mice fed ad libitum), neither control nor AgRP<sup>DTR</sup> mice showed any differences in food intake as reported previously in peripubertal mice<sup>19</sup>; here we observed diminished fasting-related hyperphagia in fasted DT-treated AgRP<sup>DTR</sup> animals compared with control animals (Fig. 4i). These data show that changes in peripheral energy metabolism alter cortical LPA levels and subsequent cortical excitability, which both appear to depend on the integrity of the AgRP circuit. Cortical hyperexcitability led to higher fasting-induced hyperphagia, while reduction of fasting-induced increase in the peripheral LPC–LPA axis—as seen in DT-treated AgRP<sup>DTR</sup> animals, which showed no cortical hyperexcitability—resulted in significant reduction of fasting-induced hyperphagia. These findings point to a body-to-brain pathway in explaining how the hypothalamus controls cortical excitability and food intake behaviours through peripheral modulation of lysophospholipid signalling (for a schematic overview of the analysed circuitry involving central–peripheral interaction see Fig. 4j).

## Discussion

It is widely accepted that changes in peripheral energy metabolism affect neuronal activity in the brain, including the cerebral cortex<sup>33</sup>. However, the molecular pathways linking changes in peripheral energy metabolism with cortical functions are not yet well understood. Based on principles of contemporary neurobiology pioneered by early-twentieth-century researchers, most notably by Santiago Ramon y Cajal<sup>34</sup>, it has been assumed that cortical functions are impacted by lower brain regions via ascending neuronal pathways originating, for example, in the hypothalamus. Indeed, increasingly sophisticated methods have been brought to bear on these issues in the past 20 years, and dozens of rigorous studies have unmasked multiple ways in which these hypothalamic neurons receiving metabolic signals forward ascending information via neuronal routes<sup>35</sup>. In relation to hunger, hypothalamic AgRP neurons have been found to play a crucial role in organization of complex behaviours<sup>19,21</sup>. In fact, our results revealed that the peripheral metabolic state under the control of hypothalamic AgRP neurons has a direct impact on cortical excitability via the LPC–LPA signalling axis (see also schematic overview in Fig. 4j). Fasting-induced cortical excitability probably resulted from peripheral adaptation of lysophospholipid metabolism, which was under the control of hypothalamic AgRP neurons. In turn, these quantitative changes in circulating lipid species, specifically LPA 18:1, themselves, served as downstream signalling molecules to align cortical adaptation to the changing metabolic state. However, there remain important questions to be resolved. For example, we do not predict that the robust phenotype triggered by adult depletion of AgRP neurons using DT can be rescued by central augmentation of LPA. Our work is not arguing for an exclusive role of the AgRP–LPA pathway in feeding control. For example, the kinetics of the rise in studied lipid species during food deprivation indicate that LPA action may not explain rapid feeding triggered by opto- or chemogenetic activation of AgRP neurons. At present, we do not know what sub-population of AgRP neurons within the arcuate nucleus is responsible for the action on LPA. Whether it is via collaterals of the same AgRP cells involved with other mechanisms of feeding control as well, or they represent a unique sub-population of AgRP neurons, will need to be determined. With that information to hand, selective manipulation of those neurons may be achieved through which we may be able

more precisely to decipher the quantitative and qualitative contribution of AgRP cells to brain functions associated with the central LPA system.

Our observations have multiple implications, and identified peripheral lipid species as potential targets for control of cortical functions in physiology and disease. In this regard, it is of interest to note that we recently showed the relevance of AgRP circuit-controlled peripheral lipid metabolism as core to short- and long-term consequences in animal models of anorexia nervosa<sup>19</sup>. Based on our current observations, we suggest that alterations in LPC and LPA species may have a direct role in the aetiology of cortical hyperexcitability in anorexia nervosa<sup>36</sup> and other psychiatric conditions associated with changes in inhibition/excitation balance as suggested by recent studies<sup>4</sup>. Our data suggest that optimization towards improved target engagement and metabolic stability of ATX inhibitors such as PF8380 might represent a starting point for the design of novel drugs supporting therapies for eating disorders. Along these lines, our studies give further support to the notion that AgRP circuit integrity is a significant contributor to healthy and diseased functions of the brain beyond feeding and energy homeostasis<sup>19–21,35</sup>. Finally, while our studies do not indicate exclusivity of the pathway, we identified a lipid-mediated control of complex behaviours. In conjunction with other work, our results suggest that the information flow between homeostatic and higher executive brain regions occurs via both ascending brain circuits and mediation of the periphery.

## Methods

**Mouse models.** All animal procedures were conducted in compliance with protocols approved by the relevant local authorities (Landesuntersuchungsamt Rheinland-Pfalz and the Institutional Animal Care and Use Committee at Yale University), and are in accordance with NIH guidelines. Mice were housed at 22–24 °C in humidity-controlled rooms (55%) with a 12/12-h light/dark cycle. Animals had ad libitum access to water and standard rodent chow (V1124–300, sniff Spezialdiäten), with the exception of the fasting experiments.

**Mouse lines.** C57Bl/6J mice were obtained from Janvier. *Lpa2*<sup>−/−</sup> male mice were generated as previously described<sup>37</sup>. The generation of male *Atx*<sup>fl/fl</sup> mice, and their genotyping, was previously described<sup>38</sup>. For cortex-specific deletion, *Atx*<sup>fl/fl</sup> animals were crossed with an *Emx1-Cre* line<sup>39</sup>. *Prp-1*<sup>R346T</sup> and *PRG-1*<sup>+/−</sup> male transgenic mice were generated as previously described and were genotyped accordingly<sup>4,4</sup>. Male and female animals expressing the human DT receptor to the *AgRP* locus (AgRP<sup>DTR</sup>) were generated as previously described<sup>29</sup>.

**Ablation of AgRP neurons.** Adult AgRP<sup>DTR</sup> animals were injected once with DT (50 µg kg<sup>−1</sup> intraperitoneally (i.p.)), diluted in sterile saline (0.9% NaCl).

**Fasting, behavioural experiments, refeeding and high-fat diet.** C57Bl/6J male animals (at least 10–12 weeks old), or genetically modified mice as indicated, were acclimatized in the facility for 7 days before the experiment and habituated to the experimental conditions. Animals analysed under different conditions were matched for weight and/or age. Experiments were performed—if not otherwise stated—during the light phase after a fasting period of at least 16–18 h (starting 1 h before beginning of the dark phase on the previous day), while water was available ad libitum. For the assessment of food consumption, food was weighed before and after an interval of 60 min for fasted mice, and during an interval of 4 h in the light phase to obtain baseline values in non-fasted mice. Behavioural analyses were performed following habituation to the test arena. Spontaneous activity was assessed using Noldus Ethovision video-tracking in the open-field arena (50 × 50 × 50 cm<sup>3</sup>; illumination 120 lux). Here, mice were placed in the centre and allowed to explore the open-field arena for 10 min. Behaviour was recorded to calculate the distance travelled. For assessment of exploratory behaviour<sup>24</sup>, animals were exposed to a novel object and interaction measured for 5 min. Exploration was defined as object investigation when the mouse's nose was within 2 cm of the object. Animals showing no interaction were excluded. A high-fat diet was provided by feeding DIO series diets from Research Diets, Inc. (D12451 (45% kcal fat) with D12450 as a control diet). Animal weight was regularly assessed, and changes were calculated to the corresponding days after starting the diet (±1 day). PF8380 was administered daily, or 3 h before testing, by i.p. injection at a concentration of 30 mg kg<sup>−1</sup> body weight (using DMSO as a vehicle) as previously described, or by daily application during administration of the high-fat diet<sup>4,40</sup>. Control animals received the vehicle DMSO.

Experimentators were blind to genotype when analysing animals of different genotypes. Experimental design figures were created with [BioRender.com](#).



**Blood plasma and CSF sample collection.** Mice were injected with a mixture of ketamine (100 mg kg<sup>-1</sup>) and xylazine (10 mg kg<sup>-1</sup>) and placed in a stereotaxic frame once deeply anaesthetized. The skin was incised to expose the skull and posterior neck muscles; the latter were divided until the cisterna magna became visible through the translucent dura mater. After cleaning away any blood residue with a cotton swab, CSF was collected using a 31-G insulin needle (Becton Dickinson) and stored at -80°C. Collection of blood plasma followed that of CSF; it was then centrifuged at 12,000g for 15 min and stored at -80°C.

**Liquid chromatography–tandem mass spectrometry analysis of LPAs and LPCs.** Analysis of LPA in blood plasma and CSF samples was performed by liquid chromatography–electrospray ionization–tandem mass spectrometry, described in detail in Supplementary Methods (ref. <sup>41</sup>). The methods were adapted to low sample sizes to allow for analysis of LPAs in individual mouse CSF samples.

**Electrophysiology.** C57Bl/6J mice, weaned around postnatal day 16 and habituated to standard chow for at least 4 days before starvation, or adult AgRP<sup>DTR</sup> animals, were used for electrophysiological analysis of either hippocampal neurons or prefrontal cortical neurons. After starvation, animals were anaesthetized with isoflurane, decapitated and brains rapidly removed and transferred to ice-cold oxygenated artificial CSF (ACSF) (in mM: 126 NaCl, 2.5 KCl, 1.25 NaH<sub>2</sub>PO<sub>4</sub>, 1 MgCl<sub>2</sub>, 2 CaCl<sub>2</sub>, 26 NaHCO<sub>3</sub>, 10 D-glucose). After cutting with a vibratome (Leica Biosystems), horizontal brain slices containing hippocampus or prefrontal cortex were equilibrated for at least 1 h. Whole-cell neuronal recordings (hippocampal CA1 neurons or layer II/III prefrontal neurons) were performed at 32°C at a holding potential of -70 mV, using patch pipettes (3–9 MΩ) filled with (in mM): 110 K-gluconate, 20 KCl, 5 NaCl, 5 EGTA, 20 K-HEPES, 0.5 CaCl<sub>2</sub>, 2 MgATP and 0.3 NaGTP. mEPSC measurements were recorded after the addition of 0.5 μM TTX and 10 μM SR-95531 to ACSF; 1 μM HA-130, 10 μM 18:0 or 18:1 LPA was then added via continuous flow as a bath application<sup>4</sup>. For analysis of mEPSCs following application of LPA 18:0 or LPA 18:1, slices were pretreated with 100 μM cyclothiazide for 30 min<sup>1</sup>. Recordings were performed using a low-pass filter at 2 kHz with an ELC-03XS amplifier (npi Electronic) and a power3 1401 A/D converter (CED), and analysed using Spike2 software (CED).

**Statistics.** Statistical analyses were performed with either GraphPad Prism software (v.9) or the BEST R package (v.4.1.2) for estimation of Bayesian posterior distribution (Supplementary Methods). Data are expressed as single values in box plots showing all data points, or as bars representing mean ± s.e.m.) with dots representing single values. Appropriate statistical tests were chosen based on the experimental condition. Following outlier identification (using ROUT or Grubbs analysis), normal distribution of data was assessed using a corresponding normality test. For data analysed with Bayesian statistical methods (using the BEST R package v.4.1.2) see Extended Data Table 1 and Supplementary Methods for details. When normal distribution was rejected, a non-parametric test was used as described. Significance was considered at P ≤ 0.05. For Bayesian posterior distribution, significance was defined as ≥80% difference between the means of group values plus effect size ≥80%, and labelled as \*; differences of means ≥90% plus effect size ≥90% were considered highly significant and labelled as \*\* (ref. <sup>42</sup>).

## References

- Trimbuch, T. et al. Synaptic PRG-1 modulates excitatory transmission via lipid phosphate-mediated signaling. *Cell* **138**, 1222–1235 (2009).
- Unichenko, P. et al. Plasticity-related gene 1 affects mouse barrel cortex function via strengthening of glutamatergic thalamocortical transmission. *Cereb. Cortex* **26**, 3260–3272 (2016).
- Vogt, J. et al. Molecular cause and functional impact of altered synaptic lipid signaling due to a prg-1 gene SNP. *EMBO Mol. Med.* **8**, 25–38 (2016).
- Thalman, C. et al. Synaptic phospholipids as a new target for cortical hyperexcitability and E/I balance in psychiatric disorders. *Mol. Psychiatry* **23**, 1699–1710 (2018).
- Moolenaar, W. H., van Meeteren, L. A. & Giepmans, B. N. The ins and outs of lysophosphatidic acid signaling. *BioEssays* **26**, 870–881 (2004).
- Yung, Y. C., Stoddard, N. C., Mirendil, H. & Chun, J. Lysophosphatidic acid signaling in the nervous system. *Neuron* **85**, 669–682 (2015).
- Yung, Y. C., Stoddard, N. C. & Chun, J. LPA receptor signaling: pharmacology, physiology, and pathophysiology. *J. Lipid Res.* **55**, 1192–1214 (2014).
- Tang, X., Benesch, M. G. & Brindley, D. N. Lipid phosphate phosphatases and their roles in mammalian physiology and pathology. *J. Lipid Res.* **56**, 2048–2060 (2015).
- Moolenaar, W. H. Lysophospholipids in the limelight: autotaxin takes center stage. *J. Cell Biol.* **158**, 197–199 (2002).
- Stracke, M. L. et al. Identification, purification, and partial sequence analysis of autotaxin, a novel motility-stimulating protein. *J. Biol. Chem.* **267**, 2524–2529 (1992).
- Hausmann, J. et al. Structural basis of substrate discrimination and integrin binding by autotaxin. *Nat. Struct. Mol. Biol.* **18**, 198–204 (2011).
- Sekas, G., Patton, G. M., Lincoln, E. C. & Robins, S. J. Origin of plasma lysophosphatidylcholine: evidence for direct hepatic secretion in the rat. *J. Lab. Clin. Med.* **105**, 190–194 (1985).
- Brindley, Hepatic secretion of lysophosphatidylcholine: a novel transport system for polyunsaturated fatty acids and choline. *J. Nutr. Biochem.* **4**, 442–449 (1993).
- Nguyen, L. N. et al. Mfsd2a is a transporter for the essential omega-3 fatty acid docosahexaenoic acid. *Nature* **509**, 503–506 (2014).
- Nakamura, K. et al. Autotaxin enzyme immunoassay in human cerebrospinal fluid samples. *Clin. Chim. Acta* **405**, 160–162 (2009).
- Sato, K. et al. Identification of autotaxin as a neurite retraction-inducing factor of PC12 cells in cerebrospinal fluid and its possible sources. *J. Neurochem.* **92**, 904–914 (2005).
- Geisler, C. E., Hepler, C., Higgins, M. R. & Renquist, B. J. Hepatic adaptations to maintain metabolic homeostasis in response to fasting and refeeding in mice. *Nutr. Metab. (Lond.)* **13**, 62 (2016).
- Joly-Amado, A. et al. Hypothalamic AgRP-neurons control peripheral substrate utilization and nutrient partitioning. *EMBO J.* **31**, 4276–4288 (2012).
- Miletta, M. C. et al. AgRP neurons control compulsive exercise and survival in an activity-based anorexia model. *Nat. Metab.* **2**, 1204–1211 (2020).
- Dietrich, M. O. et al. AgRP neurons regulate development of dopamine neuronal plasticity and nonfood-associated behaviors. *Nat. Neurosci.* **15**, 1108–1110 (2012).
- Dietrich, M. O., Zimmer, M. R., Bober, J. & Horvath, T. L. Hypothalamic AgRP neurons drive stereotypic behaviors beyond feeding. *Cell* **160**, 1222–1232 (2015).
- Schmitz, K. et al. Dysregulation of lysophosphatidic acids in multiple sclerosis and autoimmune encephalomyelitis. *Acta Neuropathol. Commun.* **5**, 42 (2017).
- Kano, K. et al. Molecular mechanism of lysophosphatidic acid-induced hypertensive response. *Sci. Rep.* **9**, 2662 (2019).
- Leger, M. et al. Object recognition test in mice. *Nat. Protoc.* **8**, 2531–2537 (2013).
- Fernandez, G. et al. Evidence supporting a role for constitutive ghrelin receptor signaling in fasting-induced hyperphagia in male mice. *Endocrinology* **159**, 1021–1034 (2018).
- He, Y. et al. A small potassium current in AgRP/NPY neurons regulates feeding behavior and energy metabolism. *Cell. Rep.* **17**, 1807–1818 (2016).
- Krizzo, J. A. et al. Regulation of locomotor activity in fed, fasted, and food-restricted mice lacking tissue-type plasminogen activator. *BMC. Physiol.* **18**, 2 (2018).
- Dunlop, K. A., Woodside, B. & Downar, J. Targeting neural endophenotypes of eating disorders with non-invasive brain stimulation. *Front. Neurosci.* **10**, 30 (2016).
- Luquet, S., Perez, F. A., Hnasko, T. S. & Palmiter, R. D. NPY/AgRP neurons are essential for feeding in adult mice but can be ablated in neonates. *Science* **310**, 683–685 (2005).
- Kaluarachchi, M. et al. A comparison of human serum and plasma metabolites using untargeted (1)H NMR spectroscopy and UPLC-MS. *Metabolomics* **14**, 32 (2018).
- Tabbai, S. et al. Effects of the LPA1 receptor deficiency and stress on the hippocampal LPA species in mice. *Front. Mol. Neurosci.* **12**, 146 (2019).
- Oliveira, T. G. et al. The impact of chronic stress on the rat brain lipidome. *Mol. Psychiatry* **21**, 80–88 (2016).
- Tataranni, P. A. et al. Neuroanatomical correlates of hunger and satiation in humans using positron emission tomography. *Proc. Natl Acad. Sci. USA* **96**, 4569–4574 (1999).
- Cajal, S. R. Y. *Textura del Sistema Nervioso del Hombre y de los Vertebrados* (Nicolás Moya, 1899).
- Waterson, M. J. & Horvath, T. L. Neuronal regulation of energy homeostasis: beyond the hypothalamus and feeding. *Cell. Metab.* **22**, 962–970 (2015).
- Focker, M. et al. Evaluation of metabolic profiles of patients with anorexia nervosa at inpatient admission, short- and long-term weight regain-descriptive and pattern analysis. *Metabolites* <https://doi.org/10.3390/metabo11010007> (2020).
- Contos, J. J. et al. Characterization of lpa(2) (Edg4) and lpa(1)/lpa(2) (Edg2/Edg4) lysophosphatidic acid receptor knockout mice: signaling deficits without obvious phenotypic abnormality attributable to lpa(2). *Mol. Cell. Biol.* **22**, 6921–6929 (2002).

38. Fotopoulou, S. et al. ATX expression and LPA signalling are vital for the development of the nervous system. *Dev. Biol.* **339**, 451–464 (2010).
39. Gorski, J. A. et al. Cortical excitatory neurons and glia, but not GABAergic neurons, are produced in the Emx1-expressing lineage. *J. Neurosci.* **22**, 6309–6314 (2002).
40. Gierse, J. et al. A novel autotaxin inhibitor reduces lysophosphatidic acid levels in plasma and the site of inflammation. *J. Pharmacol. Exp. Ther.* **334**, 310–317 (2010).
41. Brunkhorst-Kanaan, N. et al. Targeted lipidomics reveal derangement of ceramides in major depression and bipolar disorder. *Metabolism* **95**, 65–76 (2019).
42. Johnson, V. E. Revised standards for statistical evidence. *Proc. Natl Acad. Sci. USA* **110**, 19313–19317 (2013).

## Acknowledgments

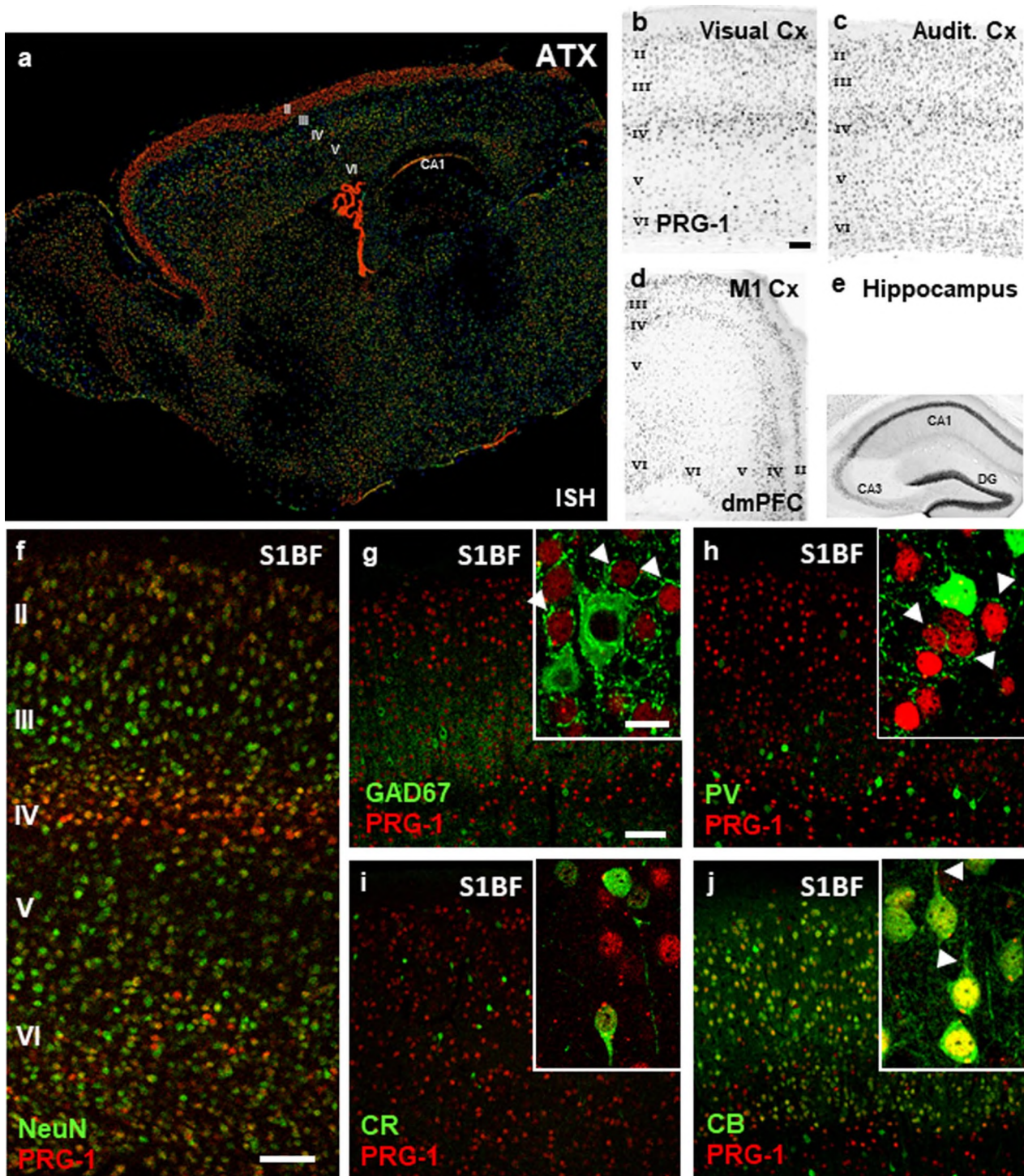
We thank C. Ernest for proofreading the manuscript. This work was supported by Deutsche Forschungsgemeinschaft (nos. FB 1039, 1080, 1193 and 1451) to J.V., R.N., I.T., F.Z. and S.G.; by Germany's Excellence Strategy (no. EXC 2030, 390661388) to J.V.; by the European Research Council (nos. ERC-AG 'LiPsyD' and ERC-PoC 'PsychAid') to R.N.; by the Boehringer-Ingelheim Foundation to J.V. and S.G.; by Stiftung Rheinland-Pfalz to J.V., R.N. and F.Z.; by InfectControl (nos. 03ZZ0826 and 03ZZ0835 to Y.L. and F.K., respectively); by the German Research Foundation (FOR2107, nos. DA1151/5-1 and DA1151/5-2 to U.D.; SFB-TRR58, nos. C09 and Z02 to U.D.); and by the Interdisciplinary Center for Clinical Research of the Medical Faculty of Münster (no. Dan3/012/17 to U.D.). SHIP is part of the Community Medicine Research net of the University of Greifswald, which receives grants from the Federal Ministry of Education and Research (nos. 01ZZ9603, 01ZZ0103 and 01ZZ0403), the Ministry of Cultural Affairs and the Social Ministry of the Federal State of Mecklenburg-West Pomerania. Genome-wide SNP typing in SHIP has been supported by a joint grant from Siemens Healthineers, Erlangen and the Federal Ministry of Education and Research (no. 03ZIK012); by the European Union and European Social Fund grant (no. EFOP-3.6.2-16-2017-0008); by an NKFIH grant (no. KKP126998) to B.R.; and by NIH grant nos. AG052005, AG067329 and DK126447 and a Klarman Family Foundation Grant to T.L.H.

## Author contributions

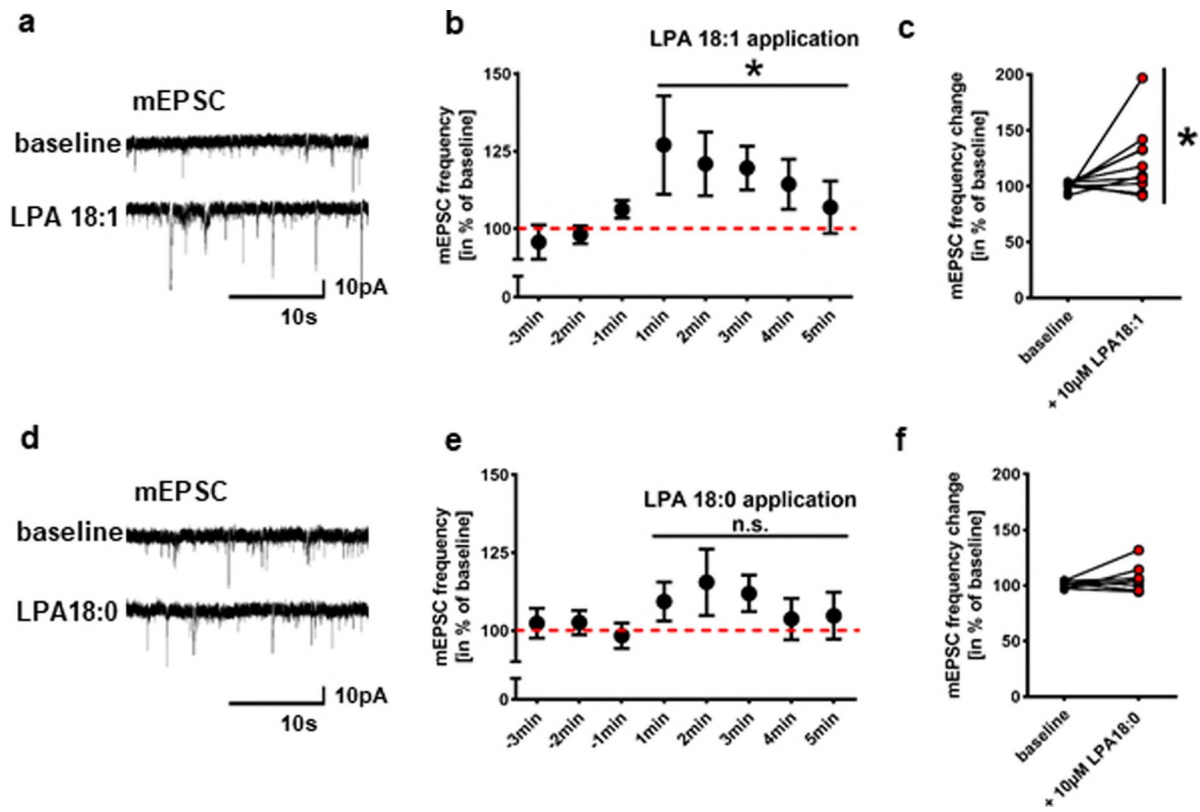
J.V., R.N. and T.L.H. designed and supervised experiments and wrote the paper. Electrophysiological and behavioural experiments were performed by H.E., B.S., Z.-W.L., M.S.-P., B.R., J.B., W.F., N.S., G.H. and K.R. I.T., Y.S., I.F.S., R.G., F.K. and Y.L. performed mass spectrometry analyses and analysed data. M.M. was involved in data analysis and statistical analysis. R.N. and F.Z. founded the Gutenberg Brain Study, which provided human data. U.D. provided human data from both the Münster Neuroimaging Cohort and the FOR2107 consortium. H.J.G. provided human data from the Study of Health in Pomerania (Ship-O and Ship-Trend). I.T., N.O., S.G., F.Z. and U.D. provided important critical input to the manuscript.

## Competing interests

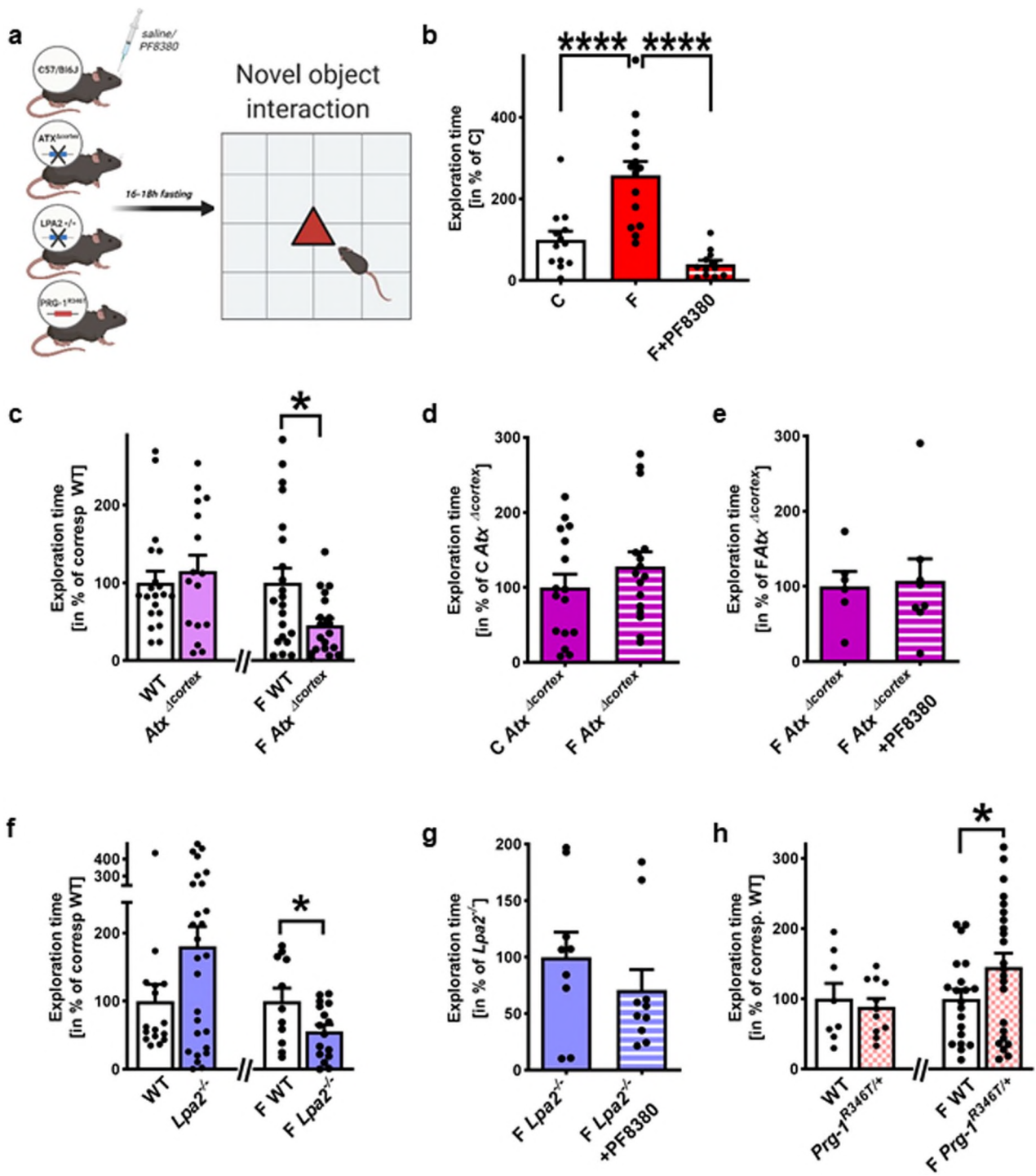
H.J.G. has received travel grants and speaker's honoraria from Fresenius Medical Care, Neuraxpharm, Servier and Janssen Cilag, as well as research funding from Fresenius Medical Care. The other authors declare no competing interests.



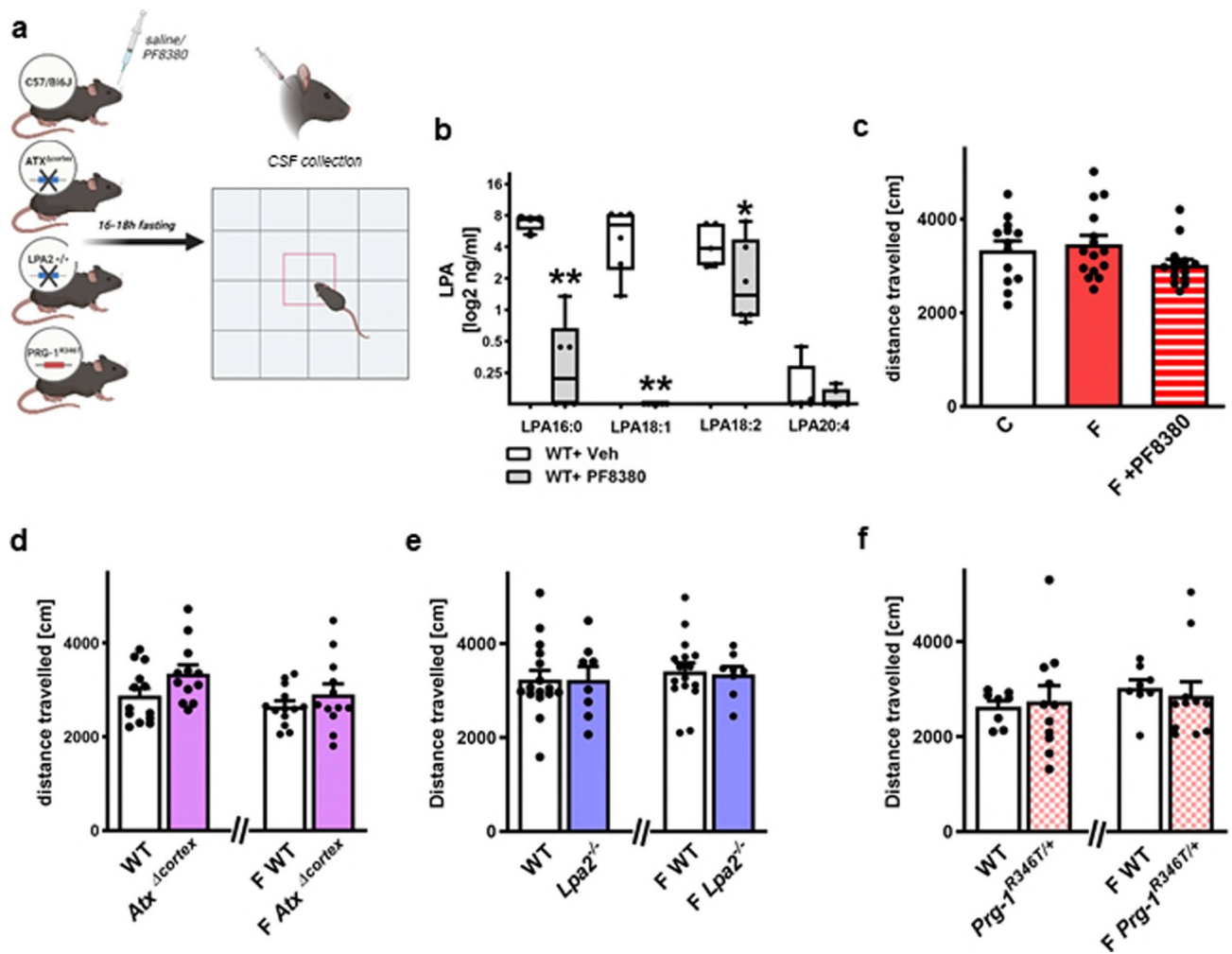
**Extended Data Fig. 1 | ATX and PRG-1 expression in cortical neurons.** **a.** *Atx* expression as shown by in-situ hybridization is present in the cortex and in the choroid ventricular plexus. Interestingly, strong expression in the cortex can be observed in the upper cortical layers (most prominent in layer II), which are important for cortical information processing. Image is adapted from the Allen Institute for Brain Science (2004). Allen Mouse Brain Atlas [532631] ([mouse.brain-map.org](http://mouse.brain-map.org)). **b-f.** PRG-1 expression, as demonstrated by the  $\beta$ -Gal reporter (for genetic details see Trimbuch et al., 2009), is predominantly found in the layers 2/3, 4 and 6 of the neocortex (visual cortex [A], auditory cortex [B], primary motor cortex [M1, C], dorsomedial prefrontal cortex [dmPFC, C] and primary sensory cortex [S1BF, F]). Strong expression was also found in the hippocampal formation (shown in E), as previously demonstrated. **g-i.** Staining for inhibitory neurons (GAD67, parvalbumin [PV] and calretinin [CR]) in the primary somatosensory cortex revealed no expression of PRG-1 in interneurons. Note the strong perisomatic inhibitory synapses of the excitatory, PRG-1-expressing neurons (arrowheads in the inserts in G and H). **j.** PRG-1 expression was detected in pyramidal (excitatory) neurons of the layer II, which express calbindin. Note the clear apical dendrites of these pyramidal neurons (arrowheads). PRG-1 expression as displayed in Fig. 1b-j was validated in at least 3 independent experiments. Scale bars: b-e 250  $\mu$ m, f-j 100  $\mu$ m, insets 15  $\mu$ m.



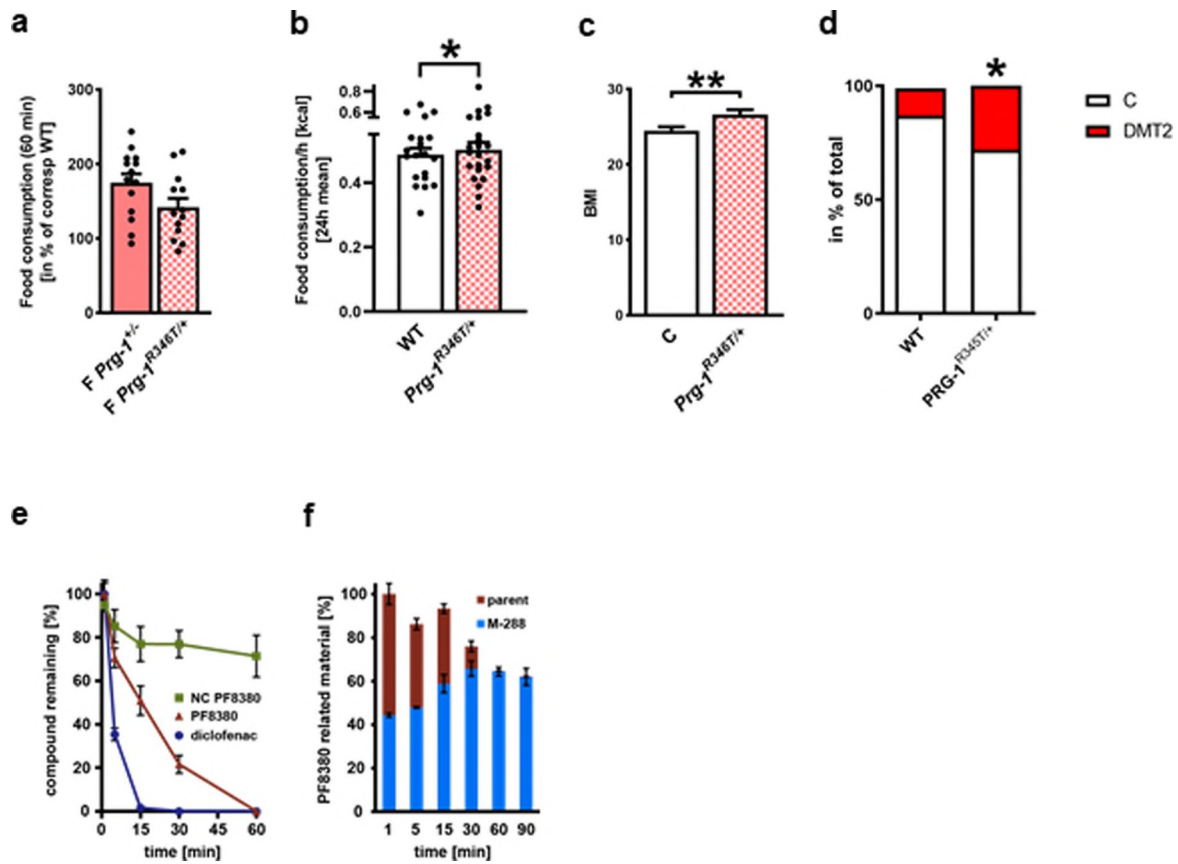
**Extended Data Fig. 2 | LPA 18:1 is a synaptic active LPA.** **a.** Original traces of patched neurons before and after LPA 18:1 application suggest higher number of miniature inward currents (mEPSCs) when compared to values before LPA 18:1 application **b.** Quantitative analysis of mEPSC frequencies following LPA 18:1 application were significantly increased when compared to baseline values before LPA 18:1 application ( $n=10$ ;  $P=0.0327$ , repeated measures one-way ANOVA). Data was calculated in % of the mean baseline over 3 min before drug application. **c.** For better evaluation, mean of the baseline of individual neurons over 3 min before LPA 18:1 stimulation was compared to that during the first 3 min after LPA 18:1 application finding significant differences ( $n=10$ ,  $P=0.027$ , two-tailed Wilcoxon matched-pairs signed rank test). **d.** Original traces before and following of LPA 18:0 application show comparable mEPSCs. **e,f.** Quantitative analysis revealed no significant effect of LPA 18:0 application on mEPSC frequency ( $n=9$ ; repeated measures one-way ANOVA). Before and after LPA 18:0 application mean values of individual neurons were calculated as described above and shown in **f** ( $n=8$ , two-tailed Wilcoxon matched-pairs signed rank test). Points and bars in **b** and **e** represent mean and s.e.m.



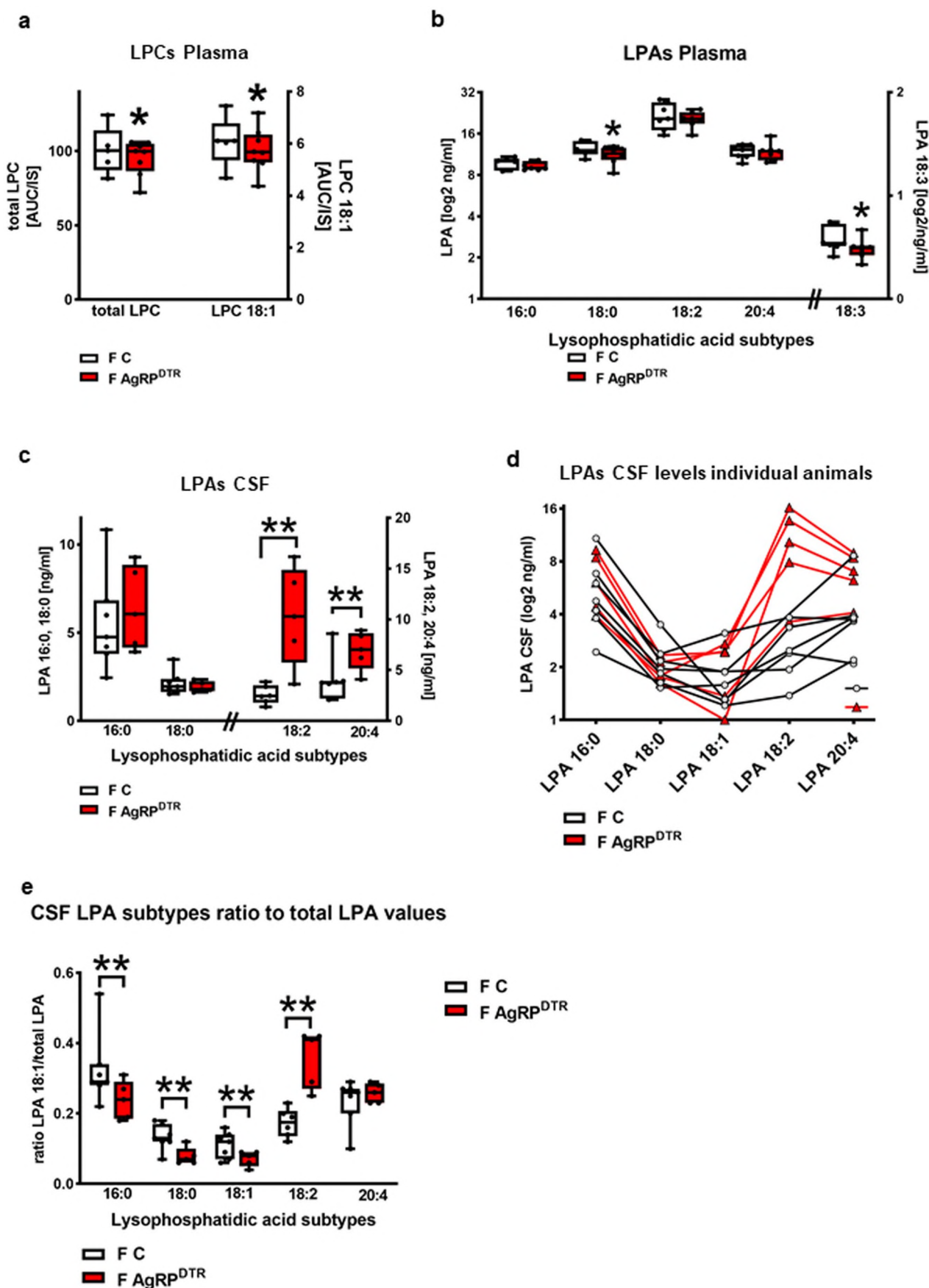
**Extended Data Fig. 3 | Fasting increases cortex-related exploratory behavior.** **a.** Experimental design. **b.** Fasting increased exploration ( $P < 0.0001$ ), which was reduced to control values by ATX inhibition ( $P < 0.0001$ ;  $n = 13$  control mice [C],  $n = 14$  fasted mice [F], and  $n = 12$  PF8380-treated fasted mice [F+PF8380]; one-way ANOVA with Bonferroni correction). **c.** Cortical ATX-deletion ( $Atx^{\Delta cortex}$ ) did not affect exploration ( $n = 20$  WT and 16  $Atx^{\Delta cortex}$  mice, two-tailed Mann-Whitney test) while it significantly reduced exploratory behavior after fasting ( $n = 21$  fasted WT [F WT] and 19 fasted  $Atx^{\Delta cortex}$  [F  $Atx^{\Delta cortex}$ ] mice;  $P = 0.0155$ , two-tailed t-test). **d.** Cortical ATX-deletion reduced fasting-induced exploration to non-fasting conditions ( $n = 16$  non-fasted mice  $Atx^{\Delta cortex}$  [C  $Atx^{\Delta cortex}$ ] mice and 16 fasted  $Atx^{\Delta cortex}$  [F  $Atx^{\Delta cortex}$ ] mice, two-tailed t-test). **e.** ATX inhibition did not alter exploratory behavior of fasted  $Atx^{\Delta cortex}$  mice ( $n = 6$  fasted  $Atx^{\Delta cortex}$  mice [F  $Atx^{\Delta cortex}$ ] and 8 fasted  $Atx^{\Delta cortex}$  + PF8380 mice [F  $Atx^{\Delta cortex}$  + PF8380], two-tailed t-test). **f.** Exploratory behavior of  $Lpa2^{-/-}$  mice under baseline conditions and after fasting ( $n = 16$  WT and  $n = 27$   $Lpa2^{-/-}$  mice, two-tailed Mann-Whitney test;  $n = 11$  fasted WT and 16 fasted  $Lpa2^{-/-}$  [F  $Lpa2^{-/-}$ ] mice,  $P = 0.032$ , two-tailed t-test). **g.** ATX inhibition by PF8380 did not alter fasting-induced exploratory behavior in  $Lpa2^{-/-}$  mice when compared to non-treated, fasted  $Lpa2^{-/-}$  mice ( $n = 9$  fasted  $Lpa2^{-/-}$  mice [F  $Lpa2^{-/-}$ ] and 10 fasted  $Lpa2^{-/-}$  + PF8380 [F  $Lpa2^{-/-}$  + PF8380] mice, two-tailed Mann-Whitney test). **h.**  $Prg-1^{R346T/+}$  mice did show normal exploratory behavior under non-fasting conditions ( $n = 8$  WT and  $n = 11$   $Prg-1^{R346T/+}$  mice, one-tailed t-test) while fasting significantly increased exploration ( $n = 20$  fasted WT [F WT] and 23 fasted  $Prg-1^{R346T/+}$  mice [F  $Prg-1^{R346T/+}$ ];  $P = 0.034$ , one-tailed t-test). Dots represent single values, bars represent mean and s.e.m., \* $p < 0.05$ , \*\*\*\* $p < 0.0001$ . Illustration was created with BioRender.



**Extended Data Fig. 4 | Overnight fasting does not alter basic locomotion.** **a.** Experimental design. **b.** PF8380 i.p. application (30 mg/kg body weight) significantly reduced LPA subtype levels in the CSF. Note that some values in the CSF after ATX inhibition by PF8380 were below the lower level of quantification and set to 0 (n=4 WT and 6 WT + PF8380 for LPA 16:0, n=6 WT and WT + PF8380 for LPA 18:1, n=5 WT and 6 WT + PF8380 for LPA 18:2 and LPA 20:4, group differences for LPA 16:0 97.6%, for LPA 18:1 99.2%, for LPA 18:2 84.5%, for LPA 20:4 69.9%, Bayesian analysis. Box plots and whiskers show data from min to max, line shows median; group differences \* >80% or \*\* >90%. **c.** Basic spontaneous motor function was not altered after fasting or after PF8380 treatment (n=13 non-fasted WT [C], 15 fasted WT [F] and n=15 fasted WT + PF8380 mice [F + PF8380], one-way ANOVA). **d.** Basic spontaneous motor function was not altered in *Atx<sup>Δcortex</sup>* mice under control conditions or after fasting [F] (n=13 WT and fasted WT [F WT] mice and n=12 *Atx<sup>Δcortex</sup>* mice [*Atx<sup>Δcortex</sup>* and F *Atx<sup>Δcortex</sup>*], two-tailed t-test). **e.** Basic spontaneous motor function was not altered in *Lpa2<sup>-/-</sup>* mice under control conditions or after fasting (n=16 WT mice [WT and F WT] and n=8 *Lpa2<sup>-/-</sup>* mice [*Lpa2<sup>-/-</sup>* and F *Lpa2<sup>-/-</sup>*], t-test). **f.** Basic spontaneous locomotion was not altered in *Prg-1<sup>R346T/+</sup>* animals under control conditions or after fasting (n=8 WT mice [WT and F WT] and n=11 *Prg-1<sup>R346T/+</sup>* mice [*Prg-1<sup>R346T/+</sup>* and F *Prg-1<sup>R346T/+</sup>*], two-tailed Mann-Whitney test). Experimental design figures were created with BioRender.com. Dots show single values and bars show mean and s.e.m. Illustration was created with BioRender.



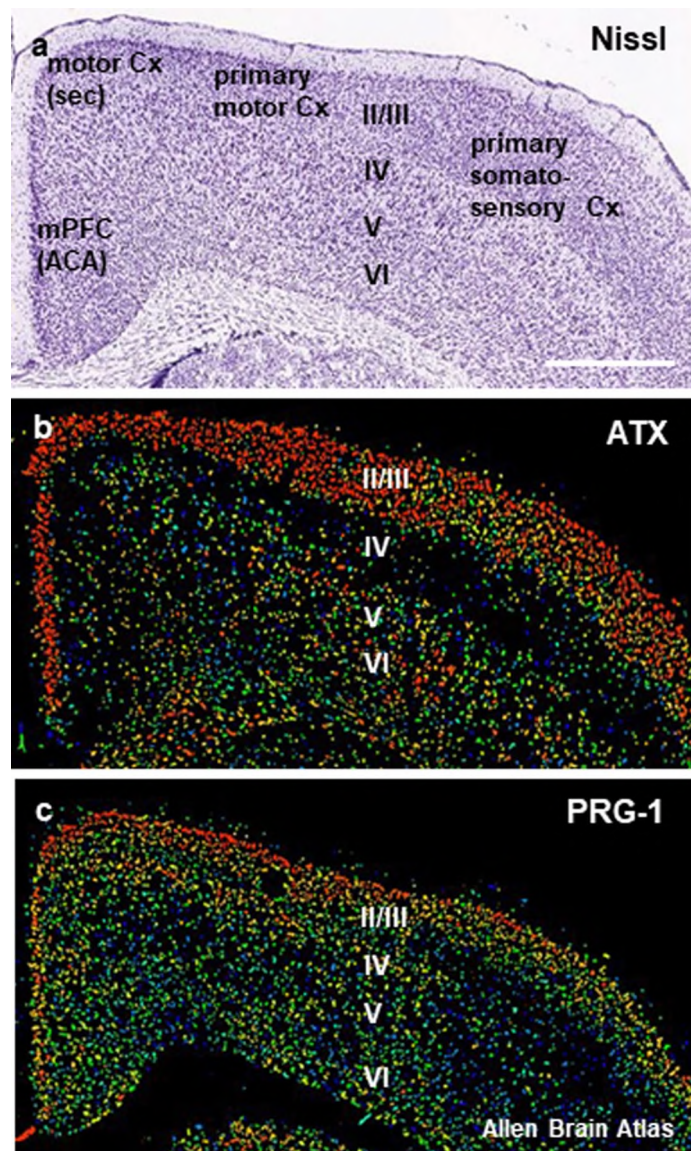
**Extended Data Fig. 5 | Altered synaptic lipid signaling is associated with increased body weight in mice and humans.** **a** Fasting-induced hyperphagia was comparable in *Prg-1*<sup>+/+</sup> and *Prg-1*<sup>R346T/+</sup> animals (n=14 F *Prg-1*<sup>+/+</sup> and n=13 F *Prg-1*<sup>R346T/+</sup>, two-sided t-test) **b** Food consumption per hour of *Prg-1*<sup>R346T/+</sup> and WT animals averaged over 24 hours (n=20 WT and n=23 *Prg-1*<sup>R346T/+</sup>, group differences 86,7%, Bayesian analysis). **c** BMI was significantly increased in human *PRG-1*<sup>R345T/+</sup> carriers (n=58 *PRG-1*<sup>R346T/+</sup> and n=60 control subjects matched for sex, age, height and education, P=0.0041, two-tailed Mann-Whitney test). **d** Diabetes type 2 (DMT2) prevalence was significantly increased in male *PRG-1*<sup>R346T/+</sup> carriers, which displayed a significantly higher odds ratio (OR) for DMT2 of 2.45 (p=0.037, logistic regression adjusted for age, sex and cohort; n=3947 control subjects with 443 individuals with diabetes; n=32 *PRG-1*<sup>R345T/+</sup> carriers with 7 individuals with diabetes; P=0.0291, chi square test, p\* < 0.05). Graph shows number of diabetic individuals as a percentage of the corresponding group. **i,j** PF8380 was quickly metabolized by human liver microsomes to a metabolite with 288 g•mol<sup>-1</sup> (n=3; CL<sub>int</sub> > 100 μl•(min•mg)<sup>-1</sup>. Diclofenac was used as a positive control. Dots show single values, bars represent mean and SEM. \*p < 0.05, \*\*\*p < 0.001, \*\*\*\*p < 0.0001, \*group differences >80% for Bayesian analysis.



Extended Data Fig. 6 | See next page for caption.



**Extended Data Fig. 6 | LPC and LPA levels in blood plasma and LPA concentrations in the CSF of fasted AgRP<sup>DTR</sup> and WT.** **a.** Blood plasma concentrations of total LPCs and 18:0 LPC in fasted AgRP<sup>DTR</sup> animals (n=5 fasted WT and n=8 fasted AgRP<sup>DTR</sup> mice, group differences 88.1% for total LPC and 86.8% for LPC 18:1, Bayesian analysis). **b.** Blood plasma levels of different LPA subtypes in fasted WT and fasted AgRP<sup>DTR</sup> animals (n=6 for LPA 16:0, 18:0 and n=7 for 18:2, 18:3 and 20:4 for fasted WT; n=8 for LPA 18:0 and 7 for all other LPA subtypes for fasted AgRP<sup>DTR</sup> animals, group differences 79.7% for LPA 16:0, 84.4% for LPA 18:0, 68.4% for LPA 18:2, 85.7% for LPA 18:3, 55.1% for LPA 20:4, Bayesian analysis). **c.** CSF levels of different LPA subtypes in fasted WT and fasted AgRP<sup>DTR</sup> mice (n=6 for LPA 18:2 and 7 for all other LPAs in fasted WT and n=5 for fasted AgRP<sup>DTR</sup> mice, group differences 68.8% for LPA 16:0, 69.4% for LPA 18:0, 97.3% for LPA 18:2, 95.5% for LPA 20:4, Bayesian analysis). **d.** Individual CSF LPA levels displayed for corresponding animals show high variance (n=6 for LPA 18:2 and 7 for all other LPAs in fasted WT and n=5 for fasted AgRP<sup>DTR</sup> mice). **e.** Ratio calculated for different LPA subtypes to total LPA levels (n=6 for LPA 18:2 and 7 for all other LPAs in fasted WT and n=5 for fasted AgRP<sup>DTR</sup> mice, group differences for LPA 16:0 90.2%, for LPA 18:0 97.5%, for LPA 18:1 93.5%, for LPA 18:2 98.8%, for LPA 20:4 70.5%, Bayesian analysis). Whiskers represent min to max, box extends from the 25<sup>th</sup> to the 75<sup>th</sup> percentile, middle line represents the median. Points represent individual values. Group differences of \* >80% or \*\* >90% are shown for Bayesian analysis.



**Extended Data Fig. 7 | Expression of synaptic lipid modulating molecules ATX and PRG-1 in the prefrontal cortex.** **a.** Nissl stained coronal section of the prefrontal cortex reaching up to the medial prefrontal cortex (mPFC, ACA anterior cingular area) and corresponding to the coronal levels of the in-situ hybridizations shown for ATX and PRG-1. Scale bar: 800  $\mu\text{m}$  **b.** ATX expression is predominantly found in the upper prefrontal cortex layers (especially in layers II/III). Data was validated in three experiments. **c.** PRG-1 is strongly expressed in the layers II/III of the prefrontal cortex but is also found at high expression levels in the layer IV. Data was validated in two experiments. Images are adapted from the Allen Institute for Brain Science (2004). Allen Mouse Brain Atlas [70613967 for *Atx* and 73992941 for *Prg-1*] ([mouse.brain-map.org](http://mouse.brain-map.org)).

**Extended Data Table 1 | Group differences calculated as differences of the means are displayed as differences between the groups, which describes the ability to separate the compared groups. Accuracy ranges for the differences of the means  $\geq 80\%$  as well as an effect size  $\geq 80\%$  were considered significant, differences of the means  $\geq 90\%$  as well as an effect size  $\geq 90\%$  were considered highly significant (Johnson 2013)**

Bayesian posterior analysis				
		group comparison	accuracy ranges of the differences of the means	significance
Fig. 1B	total LPA levels plasma	wt control vs. wt fasted	97,8%	highly significant
Fig. 1C	LPA subtypes plasma levels	wt control vs. wt fasted		
	LPA 16:0 plasma		97,1%	highly significant
	LPA 18:0 plasma		89,9%	significant
	LPA 18:2 plasma		60,9%	n.s.
	LPA 20:0 plasma		99,7%	highly significant
	LPA 20:4 plasma		99,1%	highly significant
Fig. 1D	LPA 18:1 plasma	wt control vs. wt fasted	83,8%	significant
Fig. 1E	LPA 18:1 CSF	wt control vs. wt fasted	96,4%	highly significant
Fig. 1F	LPA subtypes CSF levels	wt control vs. wt fasted		
	LPA 16:0 CSF		98,7%	highly significant
	LPA 18:0 CSF		90,3%	highly significant
	LPA 18:2 CSF		76,9%	n.s.
	LPA 20:0 CSF		60,0%	n.s.
	LPA 20:4 CSF		89,2%	significant
Fig. 4B	total LPA levels plasma	fasted control vs fasted AgRP <sup>DTR</sup>	81,0%	significant
Fig. 4C	LPA 18:1 plasma	fasted control vs fasted AgRP <sup>DTR</sup>	90,5%	highly significant
Fig. 4D	total LPA levels CSF	fasted control vs fasted AgRP <sup>DTR</sup>	92,6%	highly significant
	LPA 18:1 CSF		70,0%	n.s.
Fig. 4E	ratio LPA 18:1 / total LPA	fasted control vs fasted AgRP <sup>DTR</sup>	93,5%	highly significant
ED Fig. S4B	LPA subtypes CSF levels	wt control vs. wt + PF8380		
	LPA 16:0		97,6%	highly significant
	LPA 18:1		99,2%	highly significant
	LPA 18:2		84,5%	significant
	LPA 20:4		69,9%	n.s.
ED Fig. S5A	Food consumption	WT vs PRG-1 <sup>R346T/+</sup>	86,7%	significant
ED Fig. S6A	total LPC levels plasma	fasted control vs fasted AgRP <sup>DTR</sup>	88,1%	significant
	LPC 18:1 plasma	fasted control vs fasted AgRP <sup>DTR</sup>	86,6%	significant
ED Fig. S6B	LPA subtypes plasma levels	fasted control vs fasted AgRP <sup>DTR</sup>		
	LPA 16:0 plasma		79,7%	n.s.
	LPA 18:0 plasma		84,4%	significant
	LPA 18:2 plasma		68,4%	n.s.
	LPA18:3 plasma		85,7%	significant
	LPA 20:4 plasma		55,1%	n.s.
ED Fig. S6C	LPA subtypes CSF levels	fasted control vs fasted AgRP <sup>DTR</sup>		
	LPA 16:0 plasma		68,8%	n.s.
	LPA 18:0 plasma		69,4%	n.s.
	LPA 18:2 plasma		97,3%	highly significant
	LPA 20:4 plasma		95,5%	highly significant
ED Fig. S6E	ratio LPA subtypes / total LPA	fasted control vs fasted AgRP <sup>DTR</sup>		
	LPA 16:0 plasma		90,2%	highly significant
	LPA 18:0 plasma		97,5%	highly significant
	LPA 18:1 plasma		93,5%	highly significant
	LPA 18:2 plasma		98,8%	highly significant
	LPA 20:4 plasma		70,5%	n.s.